C.P. No. 1391

C.P. No. 1391

PROCUREMENT EXECUTIVE, MINISTRY OF DEFENCE

AERONAUTICAL RESEARCH COUNCIL

CURRENT PAPERS

A Mean Camberline Singularity Method for Two-Dimensional Steady and Oscillatory Aerofoils and Control Surfaces in Inviscid Incompressible Flow

by

B.C. Basu

Queen Mary College, London

LONDON: HER MAJESTY'S STATIONERY OFFICE

1978

£2.50 net

*CP No. 1391
October 1976

A MEAN CAMBERLINE SINGULARITY METHOD FOR TWO-DIMENSIONAL STEADY AND OSCILLATORY AEROFOILS AND CONTROL SURFACES IN INVISCID INCOMPRESSIBLE FLOW

by
B.C. Basu

SUMMARY

A numerical method has been developed to calculate the pressure distribution on the surface of steady and oscillating aerofoils in incompressible inviscid flow. In this method singularities are placed on the mean camber line of the aerofoil and the boundary condition of tangency of flow is satisfied on the surface of the aerofoil. Problems considered include steady single aerofoils with and without control surfaces, a cascade of aerofoils, aerofoils oscillating in pitch, aerofoils oscillating in heave, aerofoils in harmonic travelling gusts and control surface oscillations. Comparison with analytic solutions, and other numerical methods, where available, are good. The main advantages of this method are the relatively fast computing times and the fact that the method converges satisfactorily in the limit of zero aerofoil thickness.

---

*Replaces QMC EP-1019,. ARC 37207
(Queen Mary College, London)

NOTATION

x, z	coordinates measured along and normal to the chord line of the aerofoil
c	chord length
$\bar{x}, \bar{z}$	nondimensional coordinates relative to chord
Δ	element length of the mean camberline
$\zeta_s(x)$	steady aerofoil contour
U_∞	free stream velocity
u, w	perturbation velocity components along x and z axes
α	aerofoil incidence
δ	control surface deflection
ρ	density
Γ	circulation
σ	strength of the distributed source
γ	strength of the distributed vorticity
Q	strength of the point source
K	strength of the point vortex
ω	frequency of oscillation
$\nu(=\omega c/U_\infty)$	frequency parameter
θ	angle of pitch
h	ordinate of the heaving motion
c_p	pressure coefficient

$$C_L = \frac{\text{Lift}}{\frac{1}{2}\rho U_\infty^2 c}$$

$$C_M = \frac{\text{Moment}}{\frac{1}{2}\rho U_\infty^2 c^2}$$

$$C_H = \frac{\text{Hinge Moment}}{\frac{1}{2}\rho U_\infty^2 c^2}$$

A_{ji}, B_{ji}	influence coefficients
C_{ji}, D_{ji}	
R_{ji}, S_{ji}	
E_j, H_j	
Ci, Si	tabulated functions

Subscripts

s	steady state
o	unsteady condition
w	wake
u	upper surface
ℓ	lower surface
g	gust

1. INTRODUCTION

There are a number of well established 'exact' methods for calculating the inviscid incompressible flow around steady aerofoil sections. Some of these methods are analytic while others are numeric. Analytical methods are based on the conformal transformation technique and are restricted primarily to special aerofoil profiles. Numerical methods are based on singularity distributions and are generally applicable to both the single and multiple aerofoil problems.

A surface singularity method is one in which singularities are distributed over the aerofoil surface and the strength of the distribution is then adjusted to satisfy the boundary condition of no flow normal to the surface. The method which uses the source as the fundamental singularity is generally referred to as the A.M.O. Smith method[1]. The method which uses vorticity as the singularity was developed in Germany by Praeger[2], Martensen[3], Jacob and Riegels[4]. A further vortex singularity method has been developed more recently by Maskew[5].

In the version of the A.M.O. Smith method used at Q.M.C.[6] the aerofoil contour is represented by a series of straight line elements, on each of which is placed a uniform source distribution, the strength of which varies from element to element, and a uniform vorticity distribution which is the same for all elements. To satisfy the boundary condition of zero flow through the aerofoil contour a control point is selected at the mid-point of each element and the normal component of the total velocity (due to the free stream and source and vorticity distributions) at each control point is set to zero. The Kutta condition is satisfied by equating the downstream tangential velocities at the mid-points of the straight line elements adjacent to the trailing edge on the upper and lower surfaces. A set of linear

simultaneous equations results from which the source and vorticity distribution can be calculated.

Experience has shown that the A.M.O. Smith method gives good results except for

i) thin aerofoils (i.e. less than 5% t/c ratio)

ii) aerofoils with cusped trailing edges (e.g. all Joukowski aerofoils)

iii) highly cambered aerofoils at large C_L (refs. 7, 8)

In the numerical solution of the surface vortex distribution method, due to Jacob and Riegels[4], isolated vortices are placed at points on the aerofoil surface. The boundary condition, that the aerofoil profile be a streamline of the flow, is achieved by setting the total tangential velocity on the inside of the contour to zero at pivotal points located at the isolated vortex positions. The total velocity is the sum of the velocities induced by the surfaces vortices, plus the free stream. This inner surface tangential boundary condition, used in conjunction with a vorticity distribution, automatically satisfies the condition of zero flow through the surface for a closed body. The Kutta condition is achieved by selecting the trailing edge as one of the pivotal points and setting the vortex strength there to zero.

Maskew[5] surveyed several surface singularity models for practical aerofoil sections and concluded that the model with a linear variation of continuous vorticity along each element is the most accurate. The Kutta condition in this model is satisfied exactly at the trailing edge by setting the resultant vorticity there to zero. The method offers high accuracy in the prediction of potential flow pressure distributions over a greater range of cambers and lift coefficients than other surface singularity methods. Again the method has difficulty in handling an aerofoil with a cusped trailing edge.

One feature which is common to all surface singularity methods is the division of the aerofoil surface into a large number of elements in order to achieve the desired numerical accuracy. The number depends on the shape of the aerofoil section under consideration; for a conventional symmetrical aerofoil section of moderate thickness the number is of the order of 50 but for highly cambered aerofoils or for aerofoils with control surfaces the number needs to be as high as 200. To extend these methods directly to three dimensional problems implies extremely large numbers of elements which will lead to long computer times.

A singularity method is presented here for two dimensional aerofoils, both steady and oscillating, in an attempt to improve the efficiency of the existing surface singularity methods by reducing computer running time while maintaining the numerical accuracy over a wide range of practical problems, including the limiting case of zero thickness. The method essentially consists of distributing singularities, both source and vorticity, on the mean camber line of the aerofoil; the boundary condition of zero normal velocity is satisfied on the surface of the aerofoil.

For the steady problem the present method involves the division of the mean camber line of an aerofoil into N-straight line elements, the numbering starts from the trailing edge (Fig. 1). A small gap is left between the end of the Nth element and the leading edge of the aerofoil. On each element is placed a uniform source distribution which varies from element to element and a vorticity distribution, the strength of which varies linearly across each element. Two point sources are placed on the ends of the Nth element (closest element to the leading edge) and a point vortex on the mid-point of the Nth element. Thus, for N elements on the camber line, there are N unknown distributed source strengths, (N+1) unknown distributed vorticity strengths, two unknown point source strengths and one unknown point vortex strength, a

total of (2N+4) unknowns. These (2N+4) unknowns are determined by satisfying the boundary condition of tangency of flow at (2N+3) points on the aerofoil surface together with the appropriate Kutta condition at the trailing edge. Corresponding to the mid point of each element on the camber line two points can be defined on the upper and lower aerofoil surfaces from the intersection of normals drawn from the camber line with the aerofoil profile (see Fig. 1). This identifies 2N points on the aerofoil surface where the tangency boundary conditions are to be satisfied. Again as shown in Fig. 1 the two mid-points on the aerofoil profile in the 'gap' between the mean camber line and the leading edge, plus the leading edge point itself, give the other three points when the tangency boundary conditions are satisfied. The Kutta condition for the steady aerofoil problem is satisfied by making the strength of the vorticity at the trailing edge zero.

The above singularity model has been applied to 4% and 9.3% thick symmetrical Joukowski aerofoils at 0° and 10° incidences and to a 17.8% cambered Karman-Trefftz aerofoil at 10° incidence. The results have been compared with the exact analytic solution and the agreement is found to be excellent. The method has been applied to NACA 0012 and NLR aerofoils at incidences of 0° and 10° and to a Garabadian-Korn aerofoil at 0° and 5° incidences. The results of the present numerical method have been compared with the standard AMO Smith solution. Numerical results have also been obtained for a 4% thick symmetrical Joukowski aerofoil and 1541 section fitted with a control surface of 30% and 20% chord respectively.

The present method has also been applied to a cascade of aerofoils. A cascade of aerofoils is defined as a set of identical aerofoils equally spaced and identically oriented along an axis. Since the aerofoils are all identical, the flow and thus the source and vorticity distributions are identical. The influence coefficients are now due to a row of

of sources and vortices equally spaced along the axis. The cascade programme is capable of handling any problem in which the flow pattern repeats indefinitely along an axis. Numerical results have been obtained for NACA 0012 aerofoils in a cascade for 0° and 30° stagger angles.

The present numerical technique is extended to a two dimensional aerofoil performing harmonic variations of small amplitudes of perturbation. In the extension of the model incremental oscillatory source and vorticity distributions are situated on elements distributed over the mean steady camberline of the aerofoil super imposed on the steady source and vorticity distributions, incremental oscillatory point sources are placed at the ends of the N^{th} element and an incremental oscillatory point vortex is placed at the mid-point of the N^{th} element superimposed on the steady point sources and point vortex. An oscillatory vorticity distribution, representing the shed vorticity due to the rate of change of circulation, is placed on the mean streamline from the trailing edge. The unsteady boundary condition is satisfied on the mean steady profile. It is also assumed that the shed trailing vortex sheet is carried of with the flow at the freestream velocity. The Kutta condition is specified that the vorticity is continuous at the trailing edge.

The above mathematical model has been applied to the particular symmetrical aerofoil studied by de Vooren and de Vel[9] undergoing pitching oscillations. The numerical results for the in-phase and out-of-phase pressure distributions agree well with the results from the analytic solution.

Numerical results have been obtained for an 8.4% thick symmetrical Von Mises aerofoil and a 4% thick symmetrical Joukowski aerofoil undergoing heaving oscillations about 0° mean incidence. Comparison with the numerical solutions using an AMO Smith approach[10] is found to be good

for the Von Mises aerofoil. The results of the Joukowski aerofoil indicate that the present method converges to the linearised theory solution for vanishingly small thickness. The method has also been applied to an aerofoil in a sinusoidal vertical gust field.

The aerodynamic characteristics induced by a control surface oscillating about its hinge line have been calculated for a 4% thick symmetrical Joukowski aerofoil and a 13% thick symmetrical Karman-Trefftz aerofoil both fitted with a control surface of 30% chord. A comparison with the numerical solution of reference 10 shows reasonably good agreement for the Karman-Trefftz aerofoil. The results of the thin Joukowski aerofoil show the tendency of the present method to converge satisfactorily to the linearised theory for small thickness.

2. STEADY TWO DIMENSIONAL AEROFOIL

As shown in Fig. 2 cartesian coordinates Oxz are taken with the origin at the nose. The aerofoil chord is taken to be unity. The freestream at infinity is U_∞, inclined at an angle of incidence α to the Ox-axes.

The equation of the steady aerofoil profile relative to the axis system is denoted by

$$z_s = \zeta_s(x) \tag{1}$$

If $\bar{u}_s$ and $\bar{w}_s$ denote the perturbation velocity components on the aerofoil surface normalised with respect to U_∞ the boundary condition of tangency of flow can be written

$$\sin\alpha + \bar{w}_s = \zeta_s'(x)\ (\cos\alpha + \bar{u}_s) \tag{2}$$

where the dash denotes differentiation with respect to x.

The mean camberline of the aerofoil is divided into N straight line elements as shown in Fig. 1; numbering of the elements starts at the trailing edge and proceeds towards the leading edge. There is a

small gap between the end of the N^{th} element and the aerofoil leading edge. A uniform source distribution of strength σ_{s_i} and a vorticity distribution of strength varying linearly from γ_{s_i} to $\gamma_{s_{i+1}}$ across the element is placed on the i^{th} element. Two point sources of strengths Q_{s_1}, Q_{s_2} are placed at the ends of the N^{th} element and a point vortex of strength K_s is placed at the mid-point of the N^{th} element. Taking $\bar{\sigma}_{s_i}$, $\bar{\gamma}_{s_i}$, $\bar{Q}_{s_1}$, $\bar{Q}_{s_2}$, $\bar{K}_s$ all normalised with respect to c and U_∞, the normalised perturbation velocities at the j^{th} collocation points on the aerofoil surface due to the singularities can be expressed in the form

$$\left.\begin{aligned} \bar{u}_{s_j} &= \sum_{i=1}^{N} A_{ji}\,\bar{\sigma}_{s_i} + \sum_{i=1}^{N+1} C_{ji}\,\bar{\gamma}_{s_i} + \sum_{i=1}^{2} R_{ji}\,\bar{Q}_{s_i} + E_j\,\bar{K}_s \\ \bar{w}_{s_j} &= \sum_{i=1}^{N} B_{ji}\,\bar{\sigma}_{s_i} + \sum_{i=1}^{N+1} D_{ji}\,\bar{\gamma}_{s_i} + \sum_{i=1}^{2} S_{ji}\,\bar{Q}_{s_i} + H_j\,\bar{K}_s \end{aligned}\right\} \qquad (3)$$

A_{ji}, B_{ji}, C_{ji}, D_{ji}, R_{ji}, S_{ji}, E_j, H_j are the appropriate influence coefficients. These coefficients are given in the Appendix. The Kutta condition for the steady two dimensional flow is satisfied by making the strength of the vorticity at the trailing edge (i.e. $\bar{\gamma}_{s_1}$) zero.

The solution for the unknown variables $\bar{\sigma}_{s_i}$, $\bar{\gamma}_{s_i}$, $\bar{Q}_s$, $\bar{Q}_s$, and $\bar{K}_s$ is obtained by satisfying the boundary condition eqn. (2) at the collocation points on the aerofoil surface as indicated in Fig. 1, along with the Kutta condition of zero vorticity at the trailing edge. From the solution, $\bar{u}_{s_j}$, $\bar{w}_{s_j}$ can be reobtained using eqn. (3); the total velocity is given by

$$\bar{q}_{s_j}^{\,2} = \bar{u}_{s_j}^{\,2} + \bar{w}_{s_j}^{\,2}\,, \qquad (4)$$

and the pressure coefficient

$$c_{p_j} = 1 - \bar{q}_{s_j}^{\,2}\,. \qquad (5)$$

Total force and moment coefficients are obtained by numerical integration of the pressure coefficients.

2.1 Steady Cascade

The method described for the single aerofoil can be generalised to a cascade of identical aerofoils all with the same flow characteristics. Since each aerofoil of a cascade has the same singularity distribution the basic program for the single aerofoil only needs modification in the expression for the influence coefficients; the velocities at point in the flow due to say σ_{s_i} the source strength on the i^{th} element can be obtained by a simple summation of the appropriate influence coefficients for the contribution from each aerofoil in the cascade. In the results presented later it is assumed that the effective cascade characteristics about a typical reference aerofoil can be found by assuming 30 aerofoils above and 30 aerofoils below the reference aerofoil.

3. AEROFOILS IN SMALL AMPLITUDE SIMPLE HARMONIC MOTION

3.1 Pitching Oscillations

To extend the method described for the steady problem in Section 2 to oscillatory flow problems consider the simple harmonic pitching motion of an aerofoil, which can be superimposed on the steady profile, by

$$\theta = \theta_0 \, e^{i\omega t} \tag{6}$$

where ω is the frequency and θ_0 is the amplitude of oscillation. The point (x,z) on the aerofoil at any instant t, defined in terms of fixed axes (Fig. 3) may be expressed as

$$\left.\begin{aligned} x &= x_s + \zeta_s(x_s)\theta_0 \, e^{i\omega t} \\ z &= \zeta_s(x_s) - x_s\theta_0 \, e^{i\omega t} \end{aligned}\right\} \tag{7}$$

where θ_0 is assumed to be small, and x_s, ζ_s refer to a point on the steady mean profile.

The boundary condition for the oscillating aerofoil can be written as

$$\frac{U_\infty \sin\alpha + w - \partial z/\partial t}{U_\infty \cos\alpha + u - \partial x/\partial t} = \left(\frac{\partial z}{\partial x}\right)_{t=\text{const}} = \frac{\partial z/\partial x_s}{\partial x/\partial x_s} \quad , \tag{8}$$

where u and w are the total perturbation velocities at the surface of the aerofoil relative to fixed axes and $\partial z/\partial t$ and $\partial x/\partial t$ are the surface velocities in the z and x directions respectively. It is assumed that the variables will be composed of an oscillatory solution superimposed on the basic steady solution; the oscillatory solution is assumed to be proportional to $e^{i\omega t}$. Thus,

$$\left.\begin{aligned} u &= u_s + u_o\, e^{i\omega t} \\ w &= w_s + w_o\, e^{i\omega t} \end{aligned}\right\} \tag{9}$$

From equations (8) and (9) the following relations are obtained for the upper surface

$$\sin\alpha + \bar{w}_s = \bar{\zeta}_s'(\bar{x})(\cos\alpha + \bar{u}_s) \tag{10}$$

$$\begin{aligned} \bar{w}_o - \bar{u}_o\, \bar{\zeta}_s'(x) = -\,\theta_o\{&(\cos\alpha + \bar{u}_s) + (\sin\alpha + \bar{w}_s)\bar{\zeta}_s'(x) \\ &+ i\nu(\bar{x} + \bar{\zeta}_s(x)\zeta_s'(x)\} \quad , \end{aligned} \tag{11}$$

where $\bar{u}_s$, $\bar{w}_s$, $\bar{u}_o$, $\bar{w}_o$, are normalised perturbation velocities and $\bar{x}(=\frac{x}{c})$, $\bar{\zeta}\ (=\frac{\zeta}{c})$ are nondimensional coordinates, and ν is the nondimensional frequency parameter $(\frac{\omega c}{U_\infty})$.

According to Kelvin's circulation theorem the total circulation around a circuit in irrotational flow must be zero. Thus any change in circulation around the aerofoil must show up as shed vorticity in the wake. When the aerofoil oscillates the unsteady component of the circulation around the aerofoil $\Gamma_o e^{i\omega t}$ changes with time. It is assumed that this shed vorticity is convected along the steady trailing streamline at the

free stream velocity. The vorticity in the wake can be expressed in terms of the unsteady component of the aerofoil circulation

$$\gamma_{w_0}(x) = -\frac{i\omega\Gamma_0}{U_\infty} e^{\{-i\omega(x-x_T)/U_\infty\}} , \qquad (12)$$

where x_T refers to the trailing edge; for further details see reference (10).

In order to find a unique value of the aerofoil circulation, Γ, the Kutta condition at the trailing edge has to be applied. The Kutta condition for the present theory simply states that the vorticity is continuous at the trailing edge. It follows from the equation (12) that the vorticity at the trailing edge

$$(\gamma_0)_{t.e.} = -\frac{i\omega\Gamma_0}{U_\infty} . \qquad (13)$$

The numerical solution is outlined later in Section 3.5.

3.2 Heaving Oscillation

The formulation of the pitching oscillation problem can be easily adopted for the heaving oscillation problem by modifying the surface boundary condition.

The simple harmonic heaving motion of the aerofoil to be superimposed on the steady profile is denoted by

$$h = h_0 e^{i\omega t} . \qquad (14)$$

Following the analysis of reference (10) the boundary condition

$$\sin\alpha + \bar{w}_s = \zeta_s'(x)(\cos\alpha + \bar{u}_s) \qquad (15)$$

and

$$\bar{w}_0 - \bar{u}_0 \zeta_s'(x) = i\nu \bar{h}_0 \qquad (16)$$

3.3 Sinusoidal Gust Response

The boundary condition of the problem of an aerofoil passing through a stationary vertical gust pattern having a sinusoidal distribution of vertical velocity has been derived in reference (10). The boundary condition of this unsteady problem give the following relations

$$\sin\alpha + \bar{w}_s = \zeta_s'(x)(\cos\alpha + \bar{u}_s) \tag{17}$$

$$\bar{w}_o - \bar{u}_o\, \zeta_s'(x) = -\bar{w}_g\, e^{-i\nu\bar{x}} \tag{18}$$

where $\bar{w}_g$ is the normalised amplitude of the vertical gust velocity and $\nu = \frac{2\pi c}{\lambda}$, where λ is the spatial wavelength of the sinusoidal gust.

3.4 Control Surface Oscillation

When a control surface oscillates about its hinge the unsteady boundary condition formulated in equation (11) is applied on the part of the surface defining the control surface. On the remaining stationary surface ahead of the oscillating control surface the modified unsteady boundary condition has been derived in reference (10) and is given by

$$\bar{w}_o - \bar{u}_o\, \zeta_s'(x) = 0 \tag{19}$$

3.5 Numerical Solution

The numerical procedure is similar to the one used in solving the steady problem. The steady mean camberline of the aerofoil is divided into N-straight line elements as shown in Fig.4; numbering of the elements starts at the trailing edge and proceeds towards the leading edge. There is a small gap between the end of the N^{th} element and the aerofoil leading edge. A uniform source distribution of strength $(\sigma_{s_i} + \sigma_{o_i}\, e^{i\omega t})$ is placed on the i^{th} element together with a vorticity distribution of strength varying linearly from $(\gamma_{s_i} + \gamma_{o_i}\, e^{i\omega t})$ to $(\gamma_{s_{i+1}} + \gamma_{o_{i+1}}\, e^{i\omega t})$ across the element. Two point sources of strength

$(Q_{s_1} + Q_{o_1} e^{i\omega t})$, $(Q_{s_2} + Q_{o_2} e^{i\omega t})$ are placed at the ends of the N^{th} element and a point vortex of strength $(K_s + K_o e^{i\omega t})$ is placed at the mid-point of the N^{th} element. Because the wake extends to infinity downstream the vorticity in the wake cannot be represented by a finite number of elements. Following the procedure of reference (10) it is assumed that only the first chord length of the wake behind the trailing edge need be represented by finite elements. The effect of the remainder of the wake is calculated analytically by making the assumption that only downwash is induced at the aerofoil by this far wake. For one chord behind the aerofoil a number (M) of straight line elements are taken similar to those on aerofoil camberline and the uniform vortex strength of each of these wake elements is taken to be the vorticity strength at the centre of each element, as given by equation (12). Taking $\bar{\sigma}_{s_i}$, $\bar{\sigma}_{o_i}$, $\bar{\gamma}_{s_i}$, $\bar{\gamma}_{o_i}$, Q_{s_1}, Q_{s_2}, $\bar{Q}_{o_1}$, $\bar{Q}_{o_2}$, $\bar{K}_s$, $\bar{K}_o$ all normalised with respect to c and U_∞, the normalised perturbation velocities due to the singularities will have a steady and an oscillatory component. The steady components of the velocities will be given by equation (4), while the oscillatory components can be expressed as

$$\left.\begin{aligned} \bar{u}_{o_j} &= \sum_{i=1}^{N} A_{ji}\,\bar{\sigma}_{o_i} + \sum_{i=1}^{N+1} C_{ji}\,\bar{\gamma}_{o_i} + \sum_{i=1}^{2} R_{ji}\,\bar{Q}_{o_i} + E_j\,\bar{K}_o \\ \bar{w}_{o_j} &= \sum_{i=1}^{N} B_{ji}\,\bar{\sigma}_{o_i} + \sum_{i=1}^{N+1} D_{ji}\,\bar{\gamma}_{o_i} + \sum_{i=1}^{2} S_{ji}\,\bar{Q}_{o_i} + H_j\,\bar{K}_o \end{aligned}\right\} \qquad (20)$$

where $\bar{u}_{o_j}$, $\bar{w}_{o_j}$ are the complex velocities at the centre point of j^{th} element and A_{ji}, B_{ji}, C_{ji}, D_{ji}, R_{ji}, S_{ji}, E_j, H_j are the appropriate influence coefficients, (see Appendix). The contribution to the velocity components due to the first chord length of the wake behind the trailing edge can be expressed in the form

$$\left.\begin{aligned} \bar{u}_{o_j} &= \sum_{k=1}^{M} B_{j_k} (\bar{\gamma}_{w_o})_k = -i\nu\frac{\Gamma_o}{c} \sum_{k=1}^{M} B_{j_k} e^{-i\nu(\bar{x}_k - \bar{x}_T)} \\ \bar{w}_{o_j} &= \sum_{k=1}^{M} A_{j_k} (\bar{\gamma}_{w_o})_k = i\nu\frac{\Gamma_o}{c} \sum_{k=1}^{M} A_{j_k} e^{-i\nu(\bar{x}_k - \bar{x}_T)} \end{aligned}\right\} \quad (21)$$

The remainder of the wake aft of one chord behind the trailing edge is retained as a continuous distribution of vorticity and it is assumed to lie in the free stream direction; furthermore it is assumed that the velocity field due to this far wake is a downwash field only. The downwash field due to this far wake has been derived in reference (10) and is given as

$$\bar{w}_{o_j} = -\frac{i\nu\Gamma_o}{2\pi c} e^{-i\nu(\bar{x}_j - \bar{x}_T)} \{Ci[\nu(1 - (\bar{x}_j - \bar{x}_T))] - i[Si[\nu(1 - (\bar{x}_j - \bar{x}_T))] - \tfrac{\pi}{2}]\} \quad (22)$$

where

$$Ci(\xi) = -\int_{\xi}^{\infty} \frac{\cos\lambda}{\lambda} d\lambda$$

$$Si(\xi) = -\int_{s}^{\infty} \frac{\sin\lambda}{\lambda} d\lambda + \frac{\pi}{2} \quad ,$$

are standard tabulated functions.

The steady state solution is obtained by satisfying the steady state boundary condition at the collocation points along with the Kutta condition, as applied in the steady state. The procedure is that described in Section 2.

The unsteady problem is solved by satisfying the unsteady boundary condition, eqns.(11),or(16),or(18),or(19), at the same collocation point along with the Kutta condition, eqn. (13). The solution gives the unknown complex variables $\bar{\sigma}_{o_i}$, $\bar{\gamma}_{o_i}$, $\bar{Q}_{o_1}$, $\bar{Q}_{o_2}$ and $\bar{K}_o$ from which the unsteady velocity components are obtained using eqns. (20, 21 and 22). The calculation of the unsteady pressure coefficient c_{p_o} follows from the unsteady Bernoulli equation,

$$c_{p_o} = - 2 \bar{u}_o(\cos\alpha + \bar{u}_s) - 2 \bar{w}_o(\sin\alpha + \bar{w}_s) - \frac{2i\omega\phi_o}{U_\infty c} \qquad (23)$$

The velocity potential ϕ_o is calculated by following the procedure of reference (10). Total force and moment coefficients are obtained by numerical integration of the pressure coefficient.

A programme has been developed in FORTRAN IV for the steady problem which requires a core size of less than 20 K on the ICL 1904S, including system and programme for a problem involving 50 unknowns. For a 'clean' aerofoil of moderate thickness it has been found that about 12-14 elements on the camber line with closely spaced elements in the nose region give an accurate solution. Thus, for a lifting problem the number of unknowns is of the order of 30 and a solution on 1904S takes about 4 secs. When the aerofoil thickness is small and the aerofoil is fitted with a control surface the number of elements needs to be increased, for example, a 4% thick symmetrical Joukowski aerofoil fitted with a 30% control surface chord requires about 40 elements on the mean camberline for a reasonably accurate solution.

A separate programme has been developed in FORTRAN IV for the oscillating problem which requires a core size of just over 35 K including system and programme for 23 elements on the mean camberline (about 50 unknowns). The number of elements required for an oscillatory solution is about the same as for the steady solution except that the unknowns are now complex. Typical time for a solution involving 15 elements on the camberline (34 complex unknowns) and one frequency parameter is about 10 secs on ICL 1904S.

4. RESULTS

To check its accuracy the present method has been compared with results from analytic solutions in particular for 4% and 9.3% thick symmetrical Joukowski aerofoils at 0° and 10° incidences and to a 13%

thick, 17.8% cambered Karman-Trefftz aerofoil at 10° incidence, these are cases where the standard A.M.O. Smith method is deficient. A comparison of the numerical results derived by the present method with the exact analytic solutions are shown in Figs. 8-12. The agreement between the analytic and numerical solutions is good.

Figs. 13-18 show a comparison of the present method with the standard A.M.O. Smith method[11] for a NACA 0012, an NLR and a Garabadian-Korn aerofoil. For the NACA 0012 and NLR aerofoils 12 elements on the camberline (28 unknowns) and for the Garabadian-Korn aerofoil 10 elements (24 unknowns) have been taken. For the A.M.O. Smith method 80 surface elements (81 unknowns) were taken for both NACA 0012 and NLR aerofoils and 196 elements (197 unknowns) were taken for the Garabadian-Korn aerofoil. The numerical accuracy of the present method appears to be good for a relatively small number of unknowns.

The A.M.O. Smith method only gives the values of the flow quantities on the surface of the aerofoil at the collocation points at the mid point of elements, for any other surface locations values are obtained by interpolation. In the present method the flow quantities can be directly calculated at any point on the aerofoil surface; the values of c_p at points intermediate to collocation are shown for the NACA 0012 at 0° in Fig. 13. This is an encouraging feature of the present method.

The pressure distribution of a 4% thick symmetrical Joukowski aerofoil fitted with a 30% control surface chord and a 1541 section fitted with a 20% control surface chord have been calculated.

In Figs. 19 and 20 the overall forces and moments and the loading distribution for the 4% thick symmetrical Joukowski aerofoil fitted with a 30% control surface chord are compared with the standard linearised solution, the comparison shows that the present numerical method has the correct tendency to converge to the limit of thin aerofoil theory.

In Fig. 21 results for the 1541 section are compared with the AMO Smith solution. For the present method 13 elements on the camberline (30 unknowns) have been used for the 1541 section of which only 4 elements are on the control surface. For the AMO Smith method 156 elements have been used of which 80 elements are on the control surface. There is a small difference in the pressure distributions; which is more accurate is debatable.

Figs. 22 and 23 show the results of a NACA 0012 aerofoils in a cascade at 0° incidence and at 0° and 30° stagger. In the solution it is assumed that there are 30 aerofoils above and 30 aerofoils below.

Fig. 24 shows a comparison of the numerical oscillatory pressure distribution derived by the present method with an analytic solution obtained by De Vooren and De Vel. The comparison shows clearly that the oscillatory pressure distribution both in-phase and out-of-phase agrees well with the analytic solution.

The results of an 8.4% thick symmetrical Von Mises aerofoil and a 4% thick symmetrical Joukowski aerofoil performing a simple harmonic heaving oscillation at 0° incidence are plotted in Fig. 25. A comparison with the numerical solution[10] based on the AMO Smith approach for the Von Mises aerofoil shows that a solution using 11 elements on the camberline (26 unknowns) has a comparable accuracy using 72 surface elements (73 unknowns) for the AMO Smith solution. The numerical results for the Joukowski aerofoil when compared with the linearised theory show that the present method has the correct limiting tendency for thin aerofoils.

The results of the 8.4% thick Von Mises aerofoil and a 4% thick symmetrical Joukowski aerofoil passing through a sinusoidal (vertical) gost are plotted in Fig. 26 along with the numerical solution using the

A.M.O. Smith approach for the Von Mises aerofoil and the linearised theory solution. A comparison of the results for Von Mises aerofoil confirms that the accuracy of the present method using 11 elements on the camberline (26 unknowns) is of the same order as that of the A.M.O. Smith type solution using 72 surface elements (73 unknowns). The results of the Joukowski aerofoil when compared with the linearised theory confirms the correct behaviour for thin aerofoils.

The present method is also applied to the case of an oscillating control surface on a symmetrical Joukowski aerofoil. The results are plotted in Figs. 27 and 28 along with the A.M.O. Smith type solution for the Karman-Trefftz aerofoil and the linearised theory solution. It shows that the present method gives a solution using 14 camberline elements (32 unknowns) comparable to the A.M.O. Smith solution using 120 surface elements (121 unknowns). The results for 4% thick symmetrical aerofoil show the method has the correct tendency to converge to the linearised solution as the thickness becomes small.

5. CONCLUDING REMARKS

(a) A method has been developed for the calculation of the pressure distribution on steady and oscillating aerofoil in incompressible inviscid flow by placing the singularities on the mean camberline of the aerofoil.

(b) Satisfactory agreement has been obtained between the present numerical approach and analytic solutions.

(c) The number of unknowns in the present method is generally much less than those in the A.M.O. Smith approach for comparable accuracy. In addition the present method gives satisfactory results for thin aerofoils where the A.M.O. Smith method breaks down.

The faster method presented here is particularly advantageous for oscillatory problems.

(d) Flow quantities can be calculated directly at any point on the aerofoil surface rather than by interpolation between collocation points.

REFERENCES

1. J.L. Hess & A.M.O. Smith — Calculation of Potential Flow about Arbitrary Bodies. Progress in Aeronautical Sciences, Vol.8.

2. W. Praeger — Die Druckverteilung an Körpern in Ebener Potentialströmung, Physik. Zeilschr. XX1X, 865 (1928).

3. E. Martensen — Die Berechnung der Druckverteilung an dicken Gitterprofilen mit Hilfe von Fredholmschen Integralgleichungen Zweiter Art. AVA Nr.23, Göttingen, 1959.

4. K. Jacob and F.W. Riegels — Berechung der Druckverteilung Endlich dicker Profile ohne und mit klappen und Vortflügeln. Zeitschr. Für Flugwissensehaften, Vol.II No.9, pp. 357-367, 1963.

5. B. Maskew — A Surface Vorticity Method for Calculating the Pressure Distribution over Aerofoils of Arbitrary Thickness and Camber in Two-Dimensional Potential Flow. Department of Transport Technology, Loughborough University of Technology TT6907 (1969).

6. G.J. Hancock and G. Padfield — Numerical Solution for Steady Two-Dimensional Aerofoil in Incompressible Flow, QMC EP-1003, July 1972.

7. J.P. Giesing — Potential Flow About Two-Dimensional Aerofoils, Douglas Aircraft Company Report No.31946, 1965.

8. D.N. Foster — Note on Methods of Calculating the Pressure Distribution over the Surface of Two-Dimensional Cambered Wings, RAE TR 67095, 1967.

9. T. Theodorsen — Theory of Wing Sections of Arbitrary Shape, NACA Report 411 (1931).

10. A.I. Van de Vooren and H. Van de Vel — Unsteady Profile Theory in Incompressible Flow, Archiwum Mechaniki Stosowanej, Vol.3, No.16, 1964.

11. B.C. Basu and G.J. Hancock — Two Dimensional Aerofoils and Control Surfaces in Simple Harmonic Motion in Incompressible Inviscid Flow, QMC EP/1016/R, September 1976.

APPENDIX

SOURCE DISTRIBUTION

A source distribution on the i^{th} element between $-\frac{\Delta_i}{2} < x < \frac{\Delta_i}{2}$ (as shown in Fig. 5) with uniform normalised strength $\bar{\sigma}_i$/unit length is considered.

The velocity components δu and δw at the point (x,z) due to the small element of source distribution on $\delta\xi$ are

$$\left.\begin{aligned} \delta u(x,z) &= \frac{\bar{\sigma}_i}{2\pi}\left[\frac{x-\xi}{(x-\xi)^2+z^2}\right]\delta\xi \\ \delta w(x,z) &= \frac{\bar{\sigma}_i}{2\pi}\left[\frac{z}{(x-\xi)^2+z^2}\right]\delta\xi \end{aligned}\right\} \qquad (A.1)$$

on integration

$$u(x,z) = \frac{\bar{\sigma}_i}{4\pi}\ell n\left[\frac{(x+\frac{\Delta_i}{2})^2+z^2}{(x-\frac{\Delta_i}{2})^2+z^2}\right] = \bar{\sigma}_i\, F(x,z,\Delta_i) \qquad (A.2)$$

$$w(x,z) = \frac{\bar{\sigma}_i}{2\pi}\left[\tan^{-1}\left(\frac{x+\frac{\Delta_i}{2}}{z}\right) - \tan^{-1}\left(\frac{x-\frac{\Delta_i}{2}}{z}\right)\right] = \bar{\sigma}_i\, G(x,z,\Delta_i) \qquad (A.3)$$

In equation (A.3)

$$-\frac{\pi}{2} < \tan^{-1}\theta < \frac{\pi}{2}$$

this condition gives the correct velocity distribution i.e. antisymmetric w and symmetric u, about the x axis.

Since elements are at different orientation the problem is transformed to a fixed axis system $(\bar{x},\bar{z})$ as shown in Fig. 6; the origin of the $(\bar{x},\bar{z})$ system is taken at the leading edge.

For the source distribution along an element i the normalised velocity components $\bar{u}(\bar{x},\bar{z})$ and $\bar{w}(\bar{x},\bar{z})$ are by reference to eqns. (A.2), (A.3), now taken relative to $O\bar{x}\bar{z}$ axes

$$\left.\begin{aligned}\bar{u}(\bar{x},\bar{z}) &= \bar{\sigma}_i\{F(x,z,\Delta_i)\cos\theta \;-\; G(x,z,\Delta_i)\sin\theta\;\}\\ \bar{w}(\bar{x},\bar{z}) &= \bar{\sigma}_i\{F(x,z,\Delta_i)\sin\theta \;+\; G(x,z,\Delta_i)\cos\theta\;\}\end{aligned}\right\} \qquad (A.4)$$

when

$$\left.\begin{aligned}x &= (\bar{x} - \bar{x}_o)\cos\theta \;+\; (\bar{z} - \bar{z}_o)\sin\theta\\ z &= -\,(\bar{x} - \bar{x}_o)\sin\theta \;+\; (\bar{z} - \bar{z}_o)\cos\theta\end{aligned}\right\} \qquad (A.5)$$

The velocity components on the mid-point of the j^{th} element on the aerofoil surface due to N elements as shown in Fig. 1 is therefore written in the form

$$\begin{aligned}\bar{u}_j &= \sum_{i=1}^{N}\{F_{ji}\cos\theta_i - G_{ji}\sin\theta_i\}\,\bar{\sigma}_i\\ &= \sum_{i=1}^{N} A_{ji}\,\bar{\sigma}_i\end{aligned} \qquad (A.6)$$

$$\begin{aligned}\bar{w}_j &= \sum_{i=1}^{N}\{F_{ji}\sin\theta_i + G_{ji}\cos\theta_i\}\,\bar{\sigma}_i\\ &= \sum_{i=1}^{N} B_{ji}\,\bar{\sigma}_i\end{aligned} \qquad (A.7)$$

where

$$F_{ji} = F(\bar{x}_{ji},\bar{z}_{ji},\bar{\Delta}_i),\quad G_{ji} = G(\bar{z}_{ji},\bar{z}_{ji},\bar{\Delta}_i) \qquad (A.8)$$

where

$$\left.\begin{aligned}\bar{x}_{ji} &= \tfrac{1}{2}\{([\bar{x}_{j+1}+\bar{x}_j] - [\bar{x}_{i+1}+\bar{x}_i])\cos\theta_i + ([\bar{z}_{j+1}+\bar{z}_j] - [\bar{z}_{i+1}+\bar{z}_i])\sin\theta_i\}\\ \bar{z}_{ji} &= \tfrac{1}{2}\{-([\bar{x}_{j+1}+\bar{x}_j] - [\bar{x}_{i+1}+\bar{x}_j])\sin\theta_i + ([\bar{z}_{j+1}+\bar{z}_j] - [\bar{z}_{i+1}+\bar{z}_i]\cos\theta_i\}\\ \bar{\Delta}_i &= \{(\bar{x}_{i+1}-\bar{x}_i)^2 + (\bar{z}_{i+1}-\bar{z}_i)^2\}^{\frac{1}{2}}\\ \cos\theta_i &= \frac{\bar{x}_{i+1}-\bar{x}_i}{\bar{\Delta}_i}\;,\quad \sin\theta_i = \frac{\bar{z}_{i+1}-\bar{z}_i}{\bar{\Delta}_i}\end{aligned}\right\} \qquad (A.9)$$

LINEARLY VARYING DISTRIBUTION

A linearly varying vorticity distribution across the element i between $-\Delta_i/2 < x < \Delta_i/2$ (as shown in Fig. 7) with normalised strengths $\bar{\gamma}_i$ and $\bar{\gamma}_{i+1}$ at $x = \pm \Delta_i/2$ is considered.

The velocity components δu and δw at the point (x,z) due to the small element of vorticity distribution $\delta\bar{\xi}$ are

$$\left.\begin{aligned} \delta u &= \frac{\bar{\gamma}}{2\pi}\left[\frac{z\, d\xi}{(x-\xi)^2 + z^2}\right] \\ \delta w &= -\frac{\bar{\gamma}}{2\pi}\left[\frac{(x-\xi)d\xi}{(x-\xi)^2 + z^2}\right] \end{aligned}\right\} \qquad (A.10)$$

For the linearly varying vorticity across the element

$$\bar{\gamma} = \frac{\bar{\gamma}_{i+1} + \bar{\gamma}_i}{2} - \frac{\bar{\gamma}_{i+1} - \bar{\gamma}_i}{\Delta_i}\,\xi \qquad (A.11)$$

From (A.10), (A.11), (A.4) and (A.5)

$$\begin{aligned} \bar{u} = \frac{1}{2}\Bigg[& \bar{\gamma}_{i+1}\Big\{\Big(G(x,z,\Delta_i) + \frac{zF(x,z,\Delta_i)}{\bar{\Delta}_i/2} - \frac{xG(x,z,\Delta_i)}{\bar{\Delta}_i/2}\Big)\cos\theta \\ & + \Big(F(x,z,\Delta_i) - \frac{xF(x,z,\Delta_i)}{\bar{\Delta}_i/2} - \frac{zG(x,z,\Delta_i)}{\bar{\Delta}_i/2} - \frac{1}{\pi}\Big)\sin\theta\Big\} \\ & + \bar{\gamma}_i\Big\{\Big(G(x,z,\Delta_i) - \frac{zF(x,z,\Delta_i)}{\bar{\Delta}_i/2} + \frac{xG(x,z,\Delta_i)}{\bar{\Delta}_i/2}\Big)\cos\theta \\ & + \Big(F(x,z,\Delta_i) + \frac{xF(x,z,\Delta_i)}{\bar{\Delta}_i/2} + \frac{zG(x,z,\Delta_i)}{\bar{\Delta}_i/2} - \frac{1}{\pi}\Big)\sin\theta\Big\}\Bigg] \end{aligned} \qquad (A.12)$$

$$\bar{w} = \frac{1}{2}\Bigg|\bar{\gamma}_{i+1}\{(G(x,z,\Delta_i) + \frac{zF(x,z,\Delta_i)}{\bar{\Delta}_i/2} - \frac{xG(x,z,\Delta_i)}{\bar{\Delta}_i/2})\sin\theta_i$$

$$- (F(x,z,\Delta_i) - \frac{xF(x,z,\Delta_i)}{\bar{\Delta}_i/2} - \frac{zG(x,z,\Delta_i)}{\bar{\Delta}_i/2} - \frac{1}{\pi})\cos\theta_i\}$$

$$+ \bar{\gamma}_i\{(G(x,z,\Delta_i) - \frac{zF(x,z,\Delta_i)}{\bar{\Delta}_i/2} + \frac{xG(x,z,\Delta_i)}{\bar{\Delta}_i/2})\sin\theta_i$$

$$- (F(x,z,\Delta_i) + \frac{xF(x,z,\Delta_i)}{\bar{\Delta}_i/2} + \frac{zG(x,z,\Delta_i)}{\bar{\Delta}_i/2} - \frac{1}{\pi})\cos\theta_i\}\Bigg| \qquad (A.13)$$

The velocity components on the mid-point of element j due to N elements is written in the form

$$\bar{u}_j = \sum_{i=1}^{N} a_{ji}\,\bar{\gamma}_{i+1} + \sum_{i=1}^{N} b_{ji}\,\bar{\gamma}_i = \sum_{i=1}^{N+1} C_{ji}\,\bar{\gamma}_i \qquad (A.14)$$

$$\bar{w}_j = \sum_{i=1}^{N} c_{ji}\,\bar{\gamma}_{i+1} + \sum_{i=1}^{N} d_{ji}\,\bar{\gamma}_i = \sum_{i=1}^{N+1} D_{ji}\,\bar{\gamma}_i \qquad (A.15)$$

when

$$a_{ji} = (\frac{G_{ji}}{2} + \frac{\bar{z}_{ji}F_{ji}}{\bar{\Delta}_i} - \frac{\bar{x}_{ji}G_{ji}}{\bar{\Delta}_i})\cos\theta_i - (\frac{F_{ji}}{2} - \frac{\bar{x}_{ji}F_{ji}}{\bar{\Delta}_i} - \frac{\bar{z}_{ji}G_{ji}}{\bar{\Delta}_i} - \frac{1}{2\pi})\sin\theta_i$$

$$b_{ji} = (\frac{G_{ji}}{2} - \frac{\bar{z}_{ji}F_{ji}}{\bar{\Delta}_i} + \frac{\bar{x}_{ji}G_{ji}}{\bar{\Delta}_i})\cos\theta_i + (\frac{F_{ji}}{2} + \frac{\bar{x}_{ji}F_{ji}}{\bar{\Delta}_i} + \frac{\bar{z}_{ji}G_{ji}}{\bar{\Delta}_i} - \frac{1}{2\pi})\sin\theta_i$$

$$c_{ji} = (\frac{G_{ji}}{2} + \frac{\bar{z}_{ji}F_{ji}}{\bar{\Delta}_i} - \frac{\bar{x}_{ji}G_{ji}}{\bar{\Delta}_i})\sin\theta_i - (\frac{F_{ji}}{2} - \frac{\bar{x}_{ji}F_{ji}}{\bar{\Delta}_i} - \frac{\bar{z}_{ji}G_{ji}}{\bar{\Delta}_i} - \frac{1}{2\pi})\cos\theta_i$$

$$d_{ji} = (\frac{G_{ji}}{2} - \frac{\bar{z}_{ji}F_{ji}}{\bar{\Delta}_i} + \frac{\bar{x}_{ji}G_{ji}}{\bar{\Delta}_i})\sin\theta_i - (\frac{F_{ji}}{2} + \frac{\bar{x}_{ji}F_{ji}}{\bar{\Delta}_i} + \frac{\bar{z}_{ji}G_{ji}}{\bar{\Delta}_i} - \frac{1}{2\pi})\cos\theta_i$$

$$
\begin{aligned}
C_{ji} &= a_{ji-1} + b_{ji} \\
D_{ji} &= c_{ji-1} + d_{ji} \\
C_{j1} &= b_{j1} \\
C_{j,N+L} &= a_{j,N} \\
D_{j,1} &= d_{j,1} \\
D_{j,N+1} &= c_{j,N}
\end{aligned}
\tag{A.16}
$$

POINT SOURCE

The velocity at the mid-point of element j due to the point source of strength Q_i at $(\bar{x}_i, \bar{z}_i)$ is

$$\bar{u}_j = \frac{1}{2\pi} \frac{(\bar{x}_j - \bar{x}_i)\,\bar{Q}_i}{(\bar{x}_j - \bar{x}_i)^2 + (\bar{z}_j - \bar{z}_i)^2} = R_{ji}\,\bar{Q}_i \tag{A.17}$$

$$\bar{w}_j = \frac{1}{2\pi} \frac{(\bar{z}_j - \bar{z}_i)\,\bar{Q}_i}{(\bar{x}_j - \bar{x}_i)^2 + (\bar{z}_j - \bar{z}_i)^2} = S_{ji}\,\bar{Q}_i \tag{A.18}$$

POINT VORTEX

The velocity at the mid-point of element j due to the point vortex of strength K at $(\bar{x},\bar{z})$ is

$$\bar{u}_j = \frac{1}{2\pi} \frac{(\bar{z}_j - \bar{z})\,\bar{K}}{(\bar{x}_j - \bar{x})^2 + (\bar{z}_j - \bar{z})^2} = E_j\,\bar{K} \tag{A.19}$$

$$\bar{w}_j = -\frac{1}{2\pi} \frac{(\bar{x}_j - \bar{x})\,\bar{K}}{(\bar{x}_j - \bar{x})^2 + (\bar{z}_j - \bar{z})^2} = H_j\,\bar{K} \tag{A.20}$$

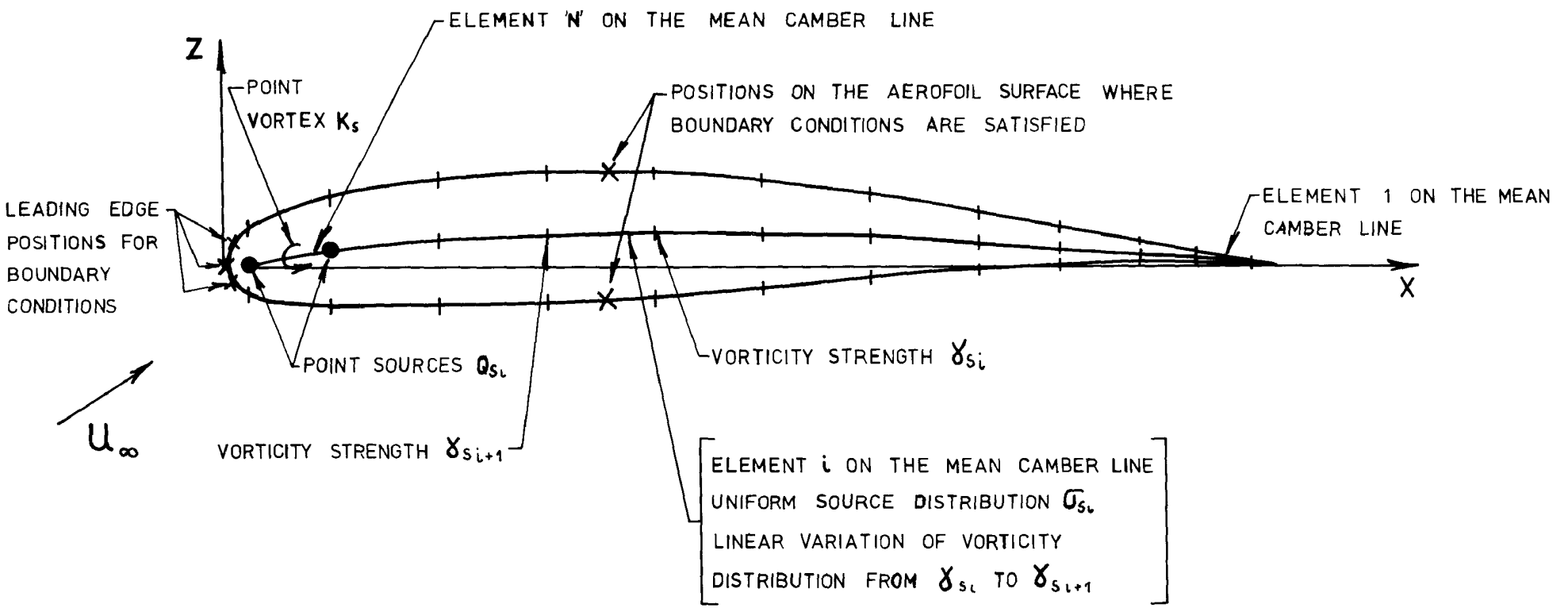

MATHEMATICAL MODEL IN STEADY FLOW

Fig. 1

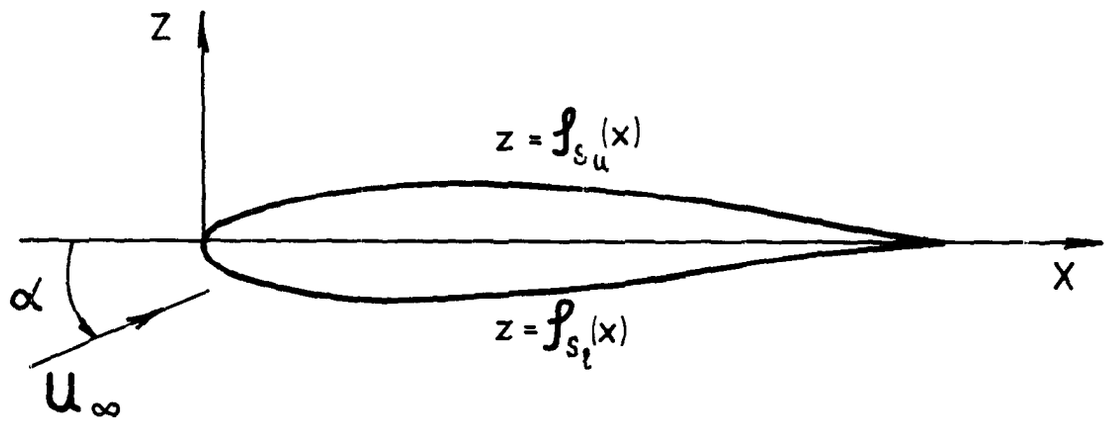

GENERAL NOTATION

Fig. 2

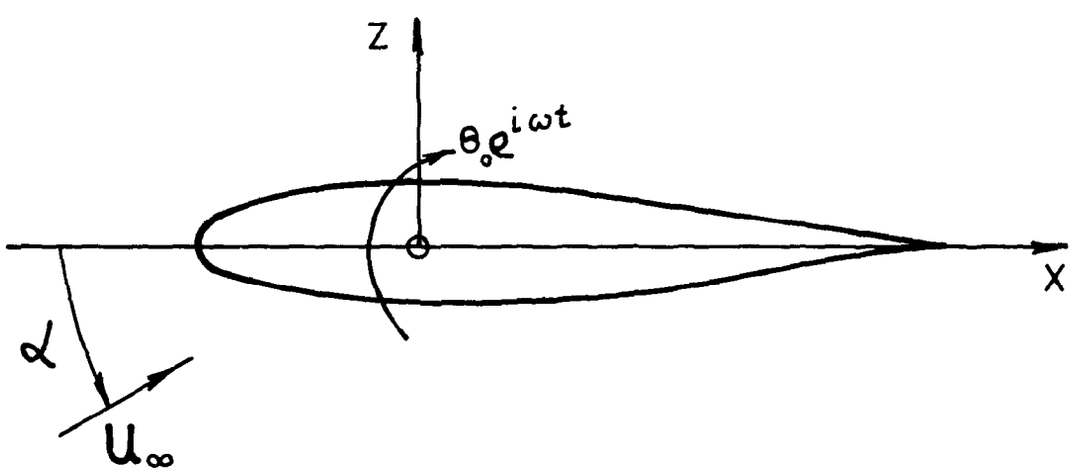

NOTATION FOR OSCILLATING AEROFOIL

Fig. 3

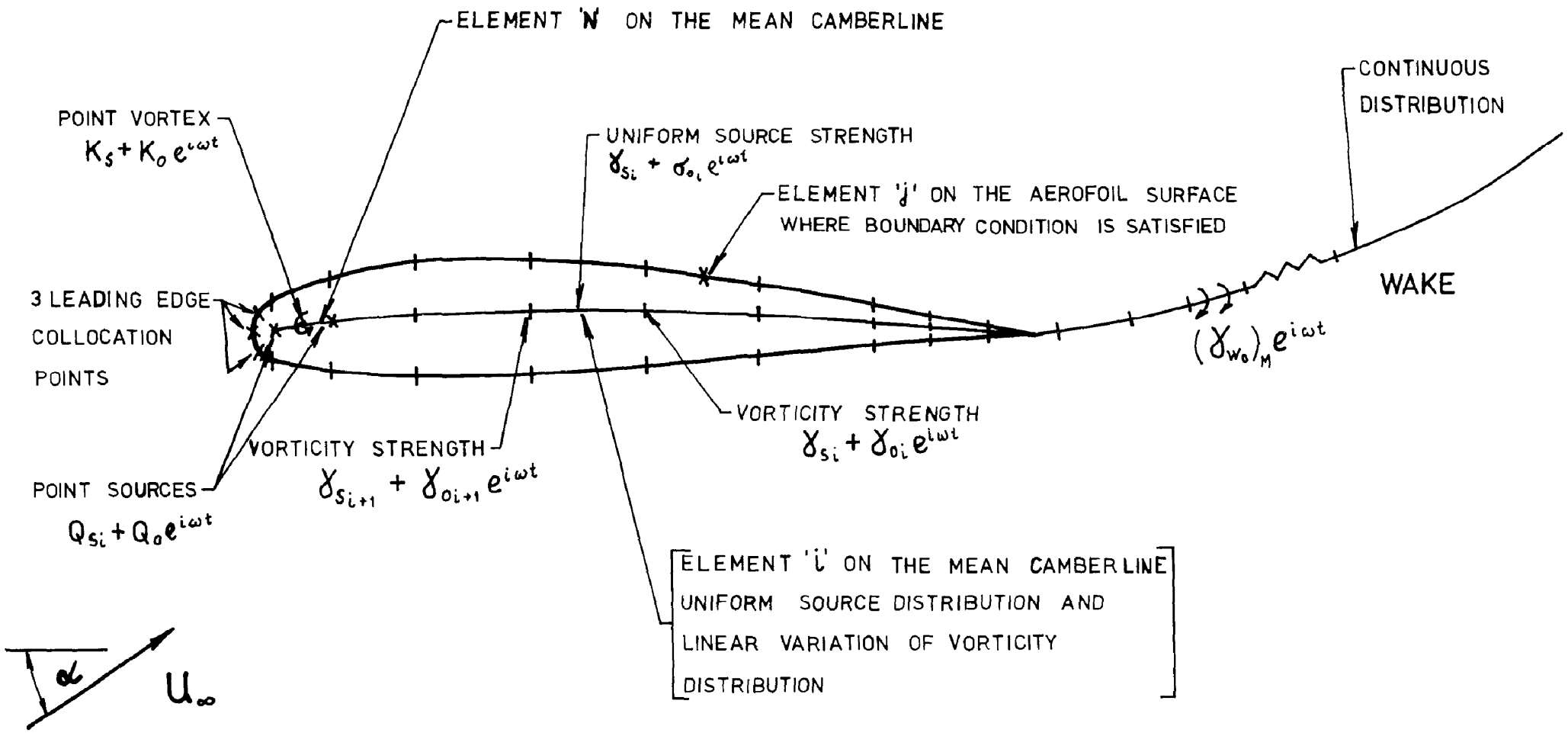

MATHEMATICAL MODEL OF AN OSCILLATING AEROFOIL

Fig. 4

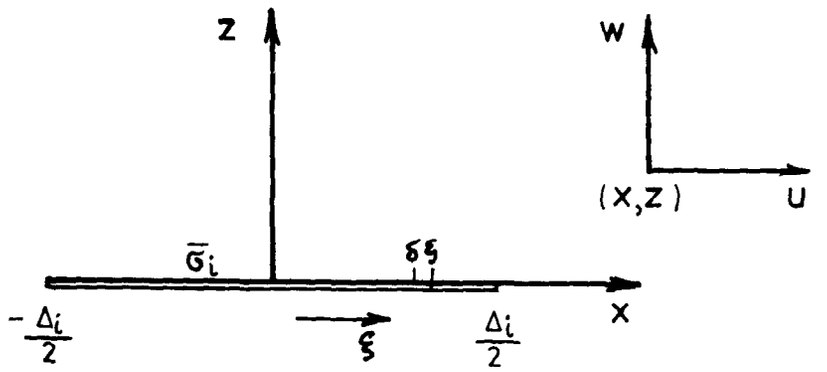

SOURCE ELEMENT ON ELEMENT i

Fig. 5

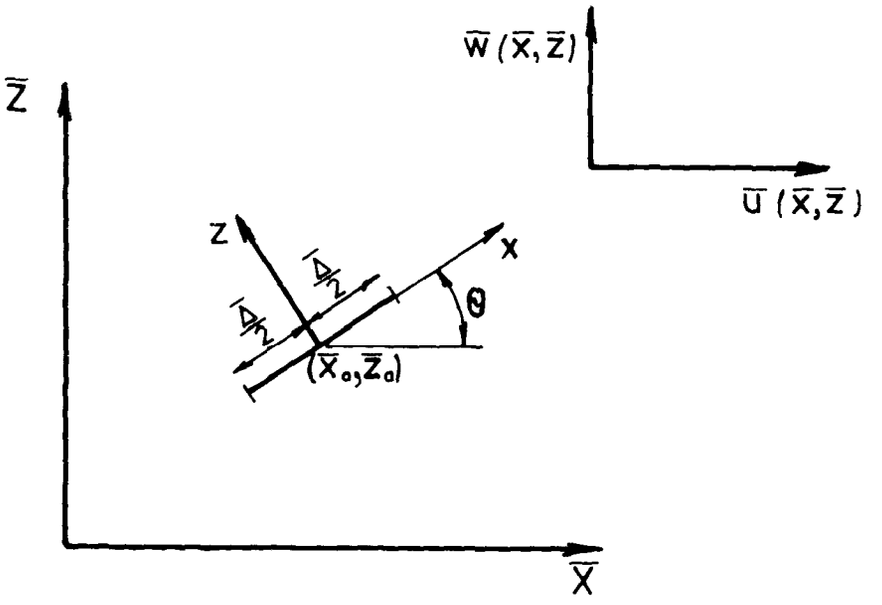

AXES SYSTEM

Fig. 6

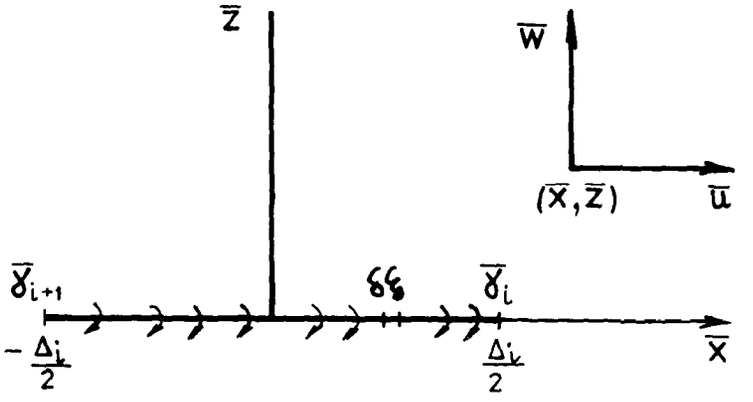

LINEAR VARIATION OF VORTICITY DISTRIBUTION ON ELEMENT i

Fig. 7

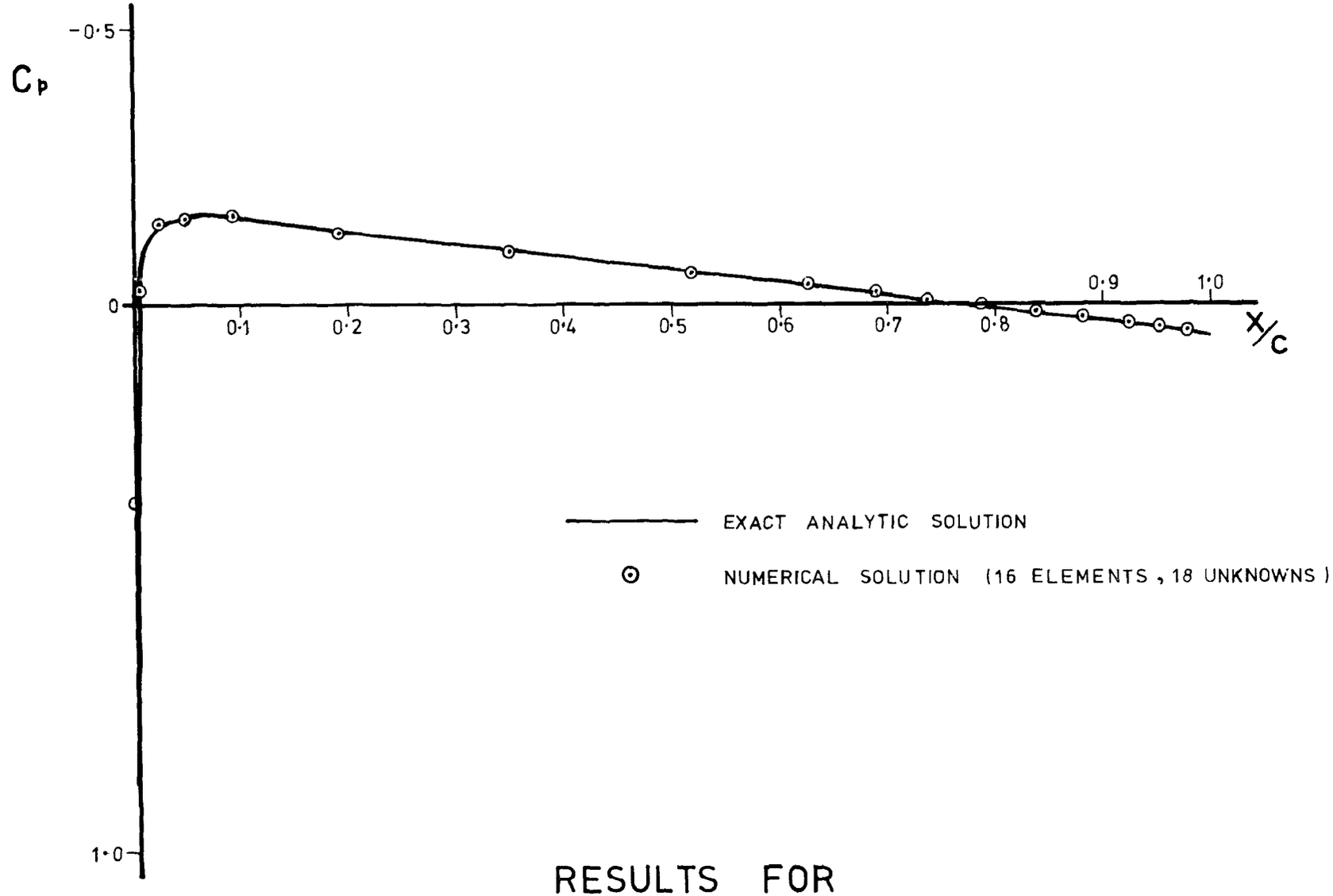

RESULTS FOR

4 % THICK SYMMETRICAL JOUKOWSKI AEROFOIL

AT 0° INCIDENCE

Fig. 8

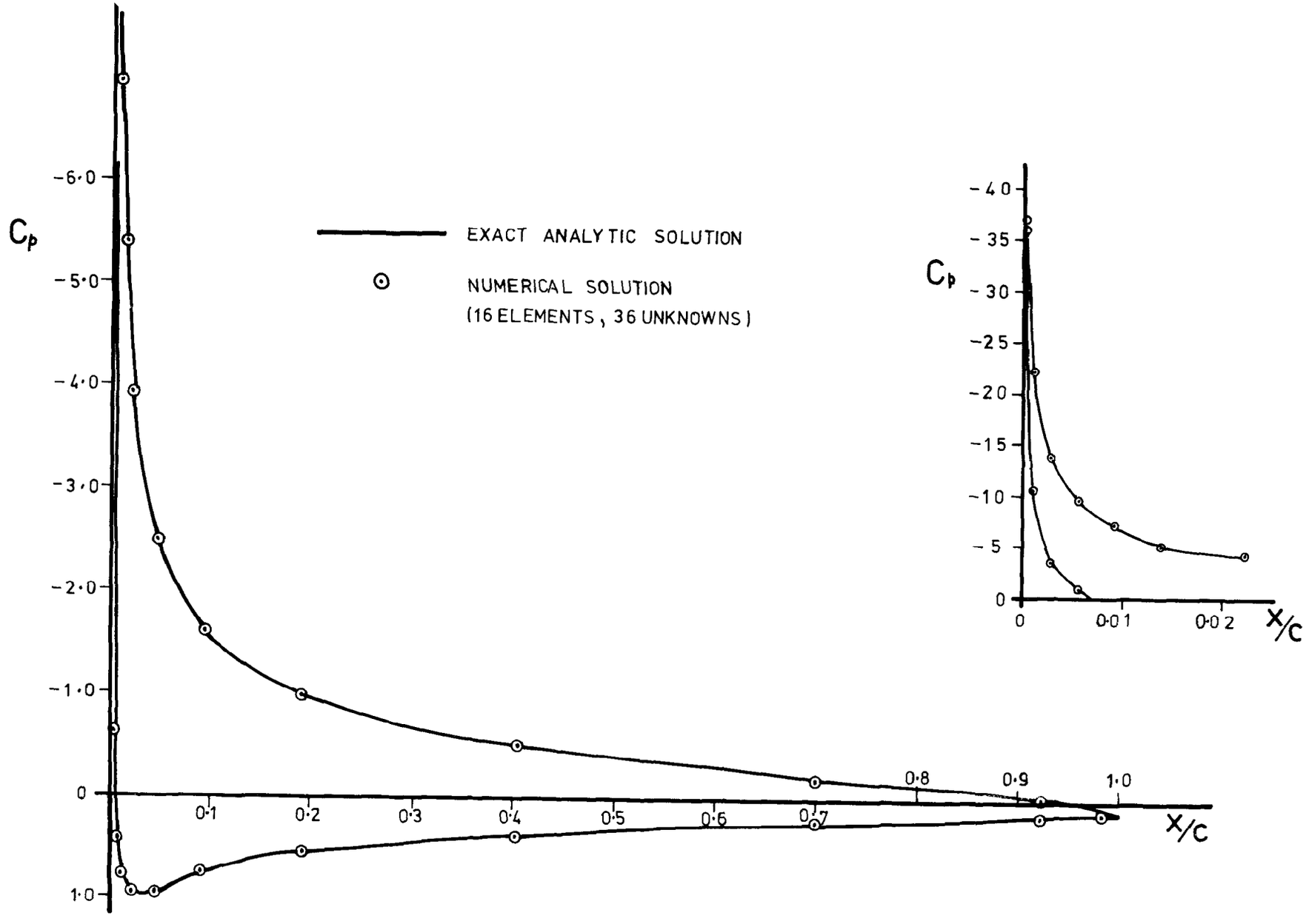

RESULTS FOR 4% THICK SYMMETRICAL JOUKOWSKI AEROFOIL AT 10° INCIDENCE

Fig. 9

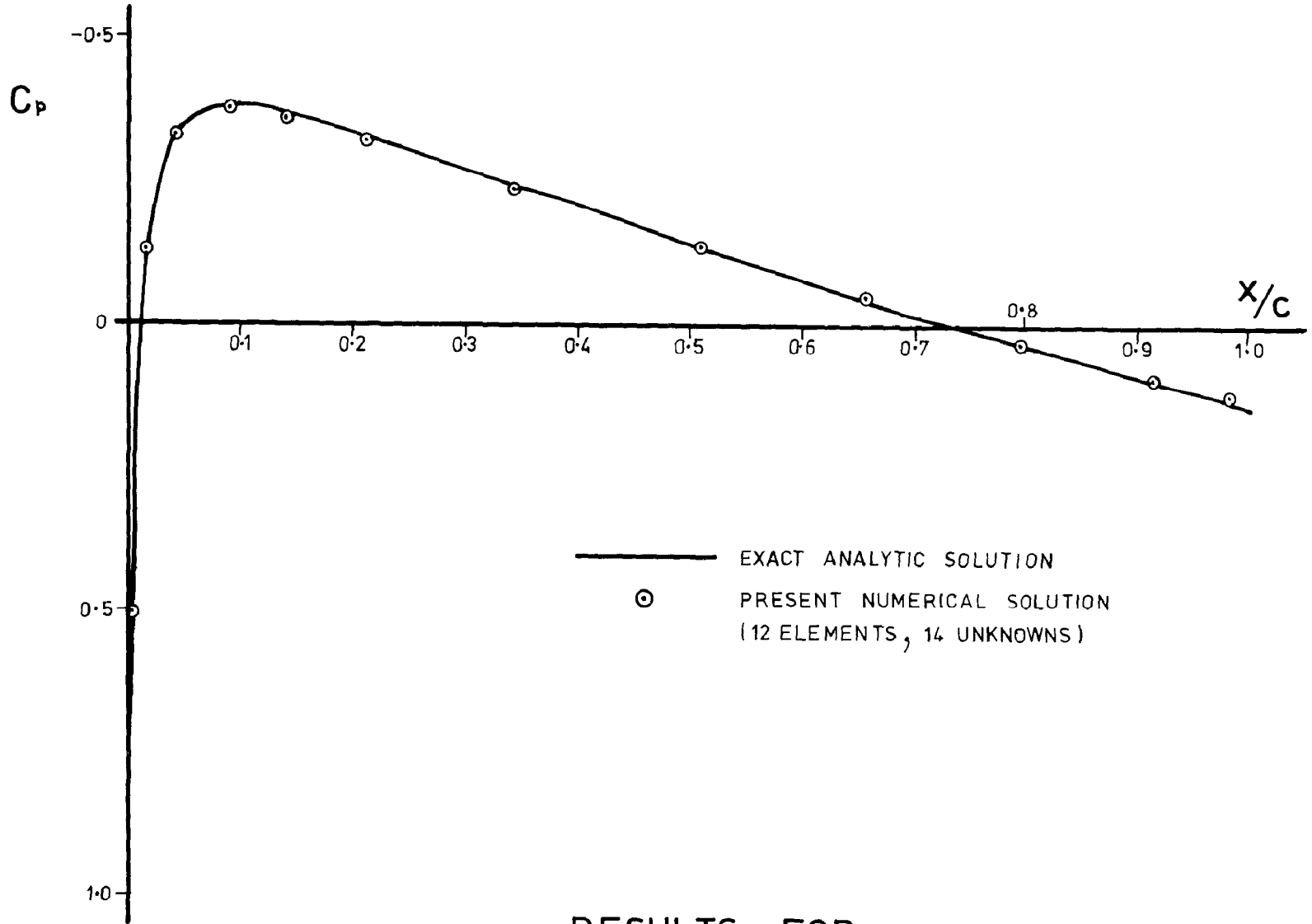

RESULTS FOR
9·3 % THICK SYMMETRICAL JOUKOWSKI AEROFOIL
AT 0° INCIDENCE

Fig. 10

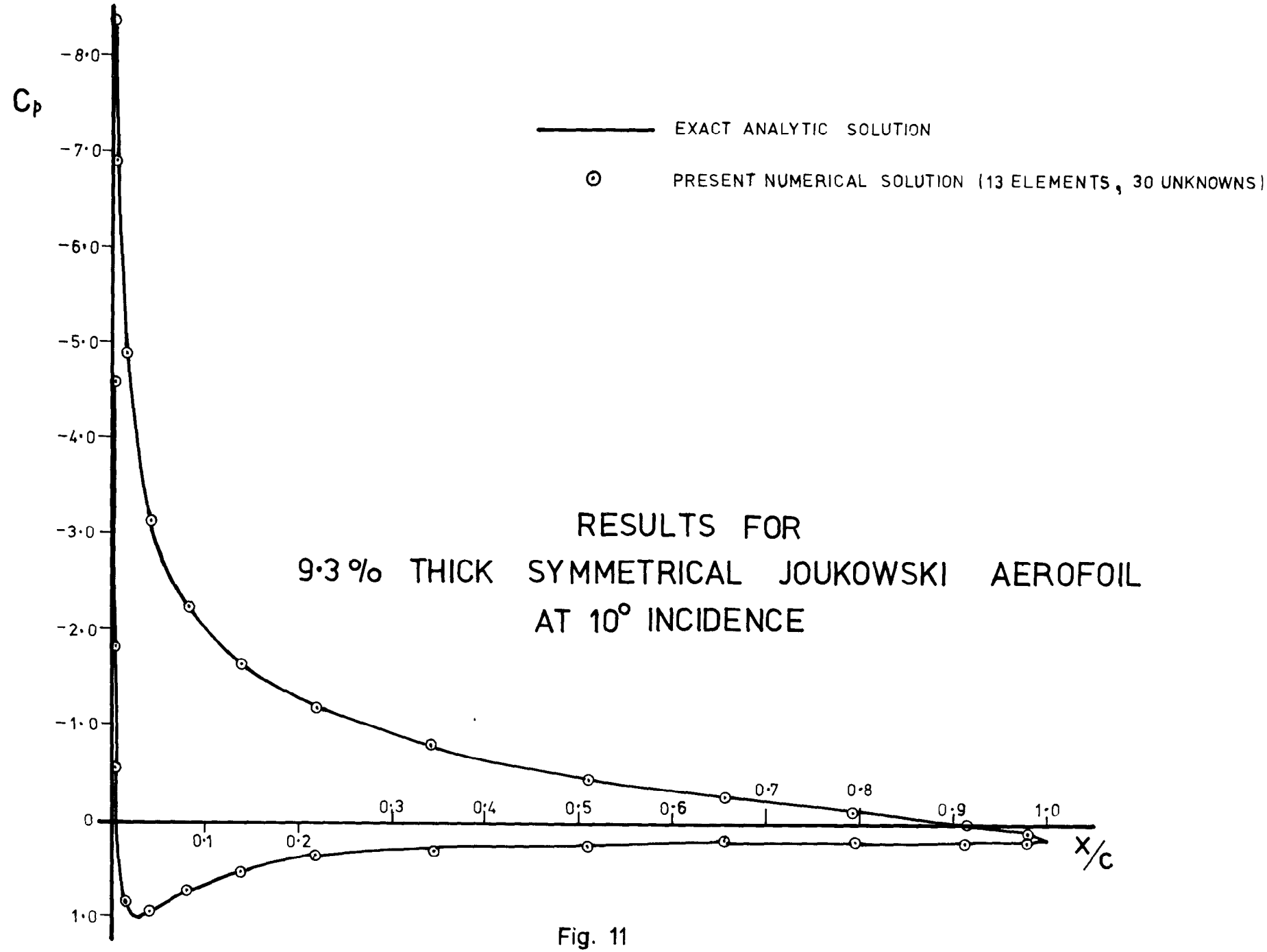
C_p
-8·0
-7·0
-6·0
-5·0
-4·0
-3·0
-2·0
-1·0
0
1·0
EXACT ANALYTIC SOLUTION
PRESENT NUMERICAL SOLUTION (13 ELEMENTS, 30 UNKNOWNS)
RESULTS FOR
9·3 % THICK SYMMETRICAL JOUKOWSKI AEROFOIL
AT 10° INCIDENCE
0·1
0·2
0·3
0·4
0·5
0·6
0·7
0·8
0·9
1·0
X/c

Fig. 11

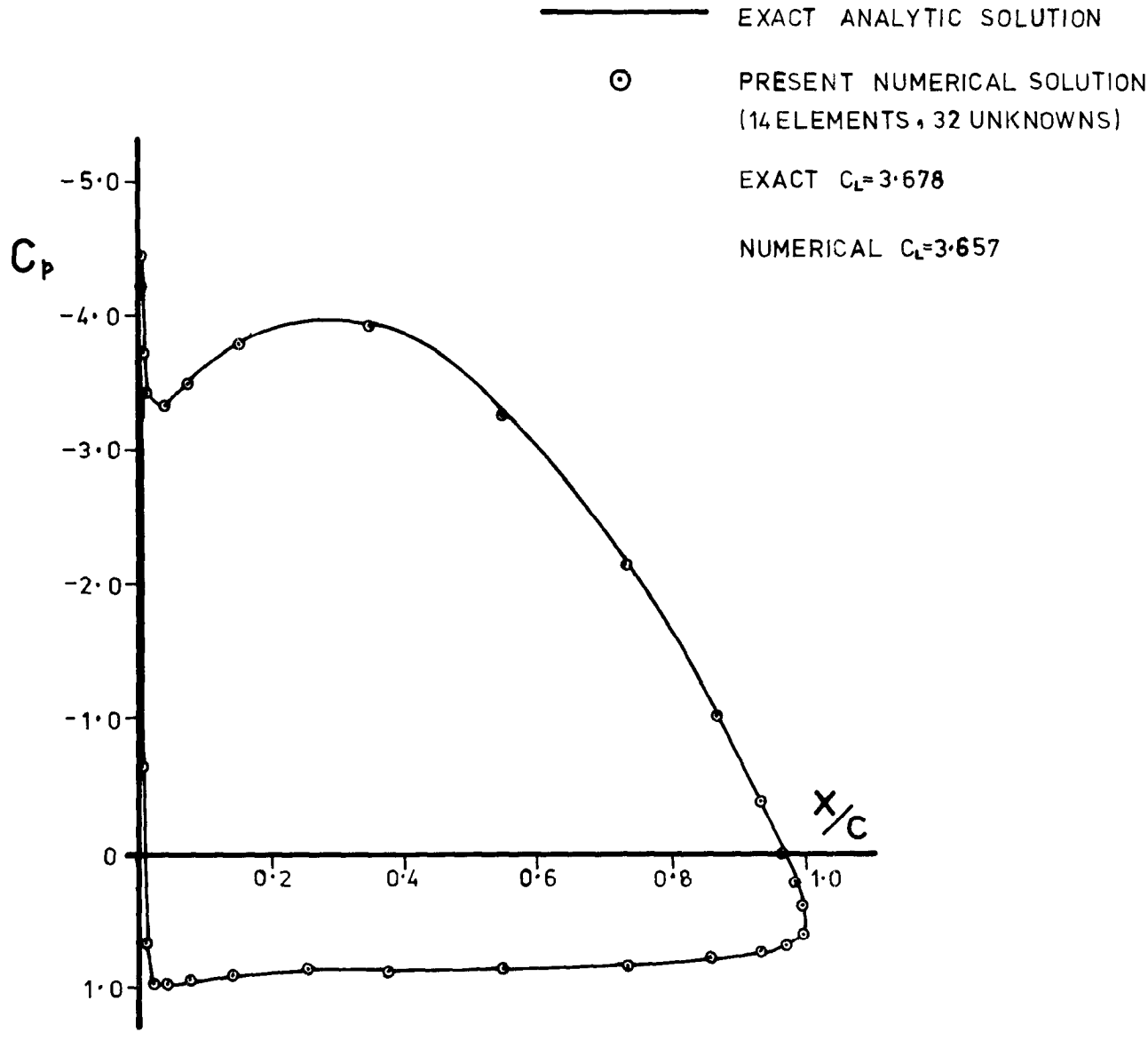

RESULTS FOR
17·8 % CAMBERED KARMAN-TREFFTZ AEROFOIL
AT 10° INCIDENCE

Fig. 12

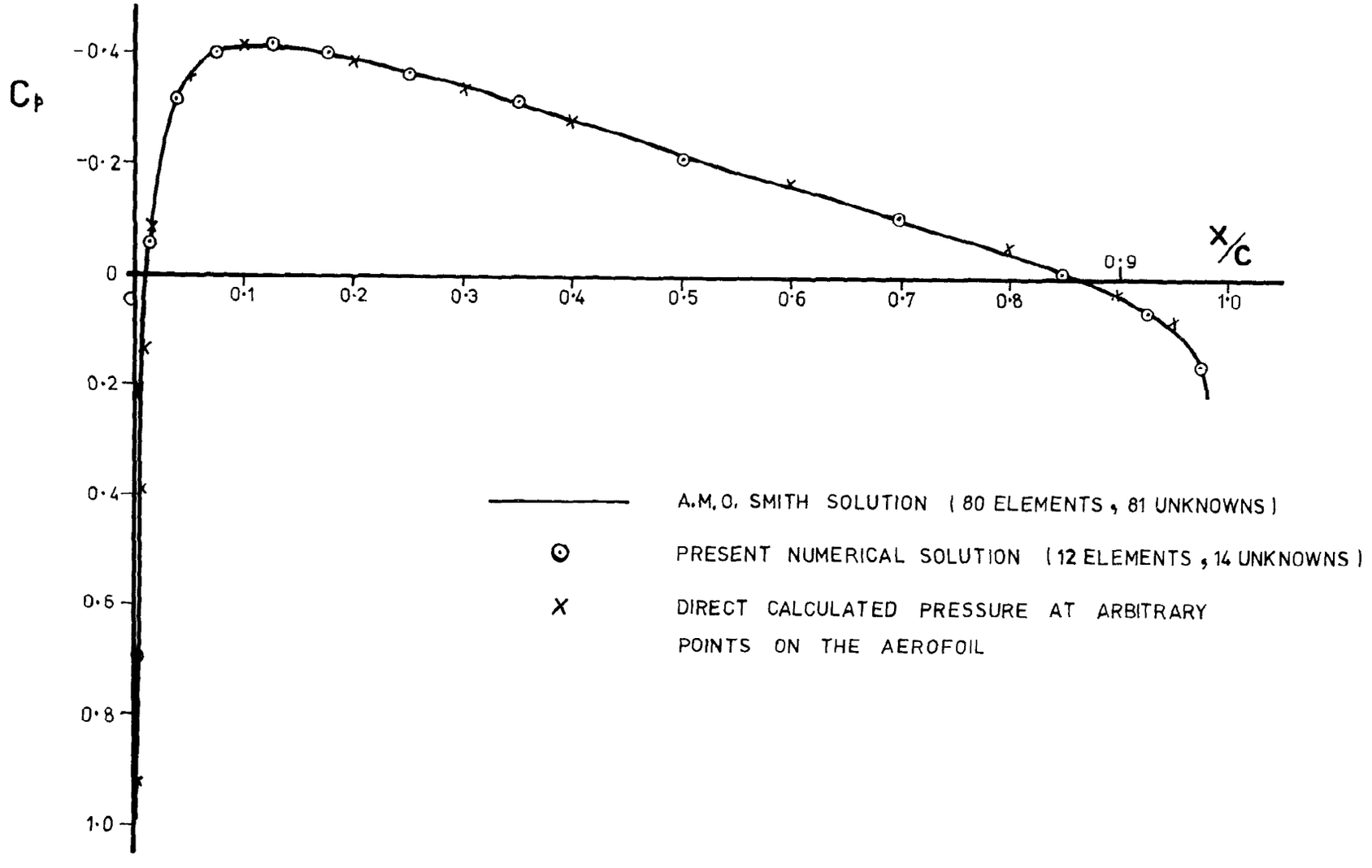

COMPARISON OF PRESENT NUMERICAL SOLUTION WITH THE A.M.O. SMITH SOLUTION

NACA 0012 AT 0° INCIDENCE

Fig. 13

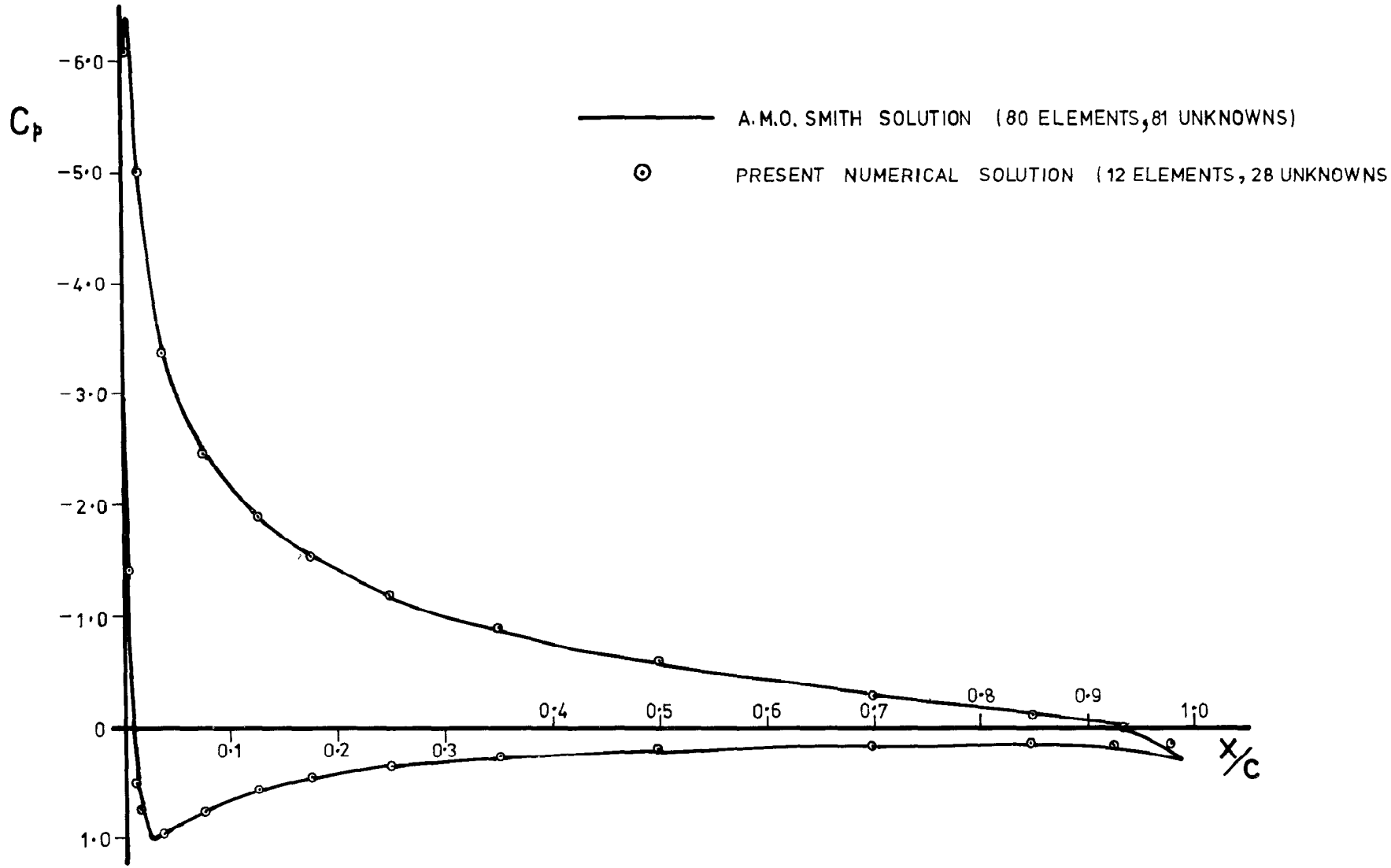

COMPARISON OF PRESENT NUMERICAL SOLUTION WITH THE A.M.O. SMITH SOLUTION

NACA 0012 AT 10° INCIDENCE

Fig. 14

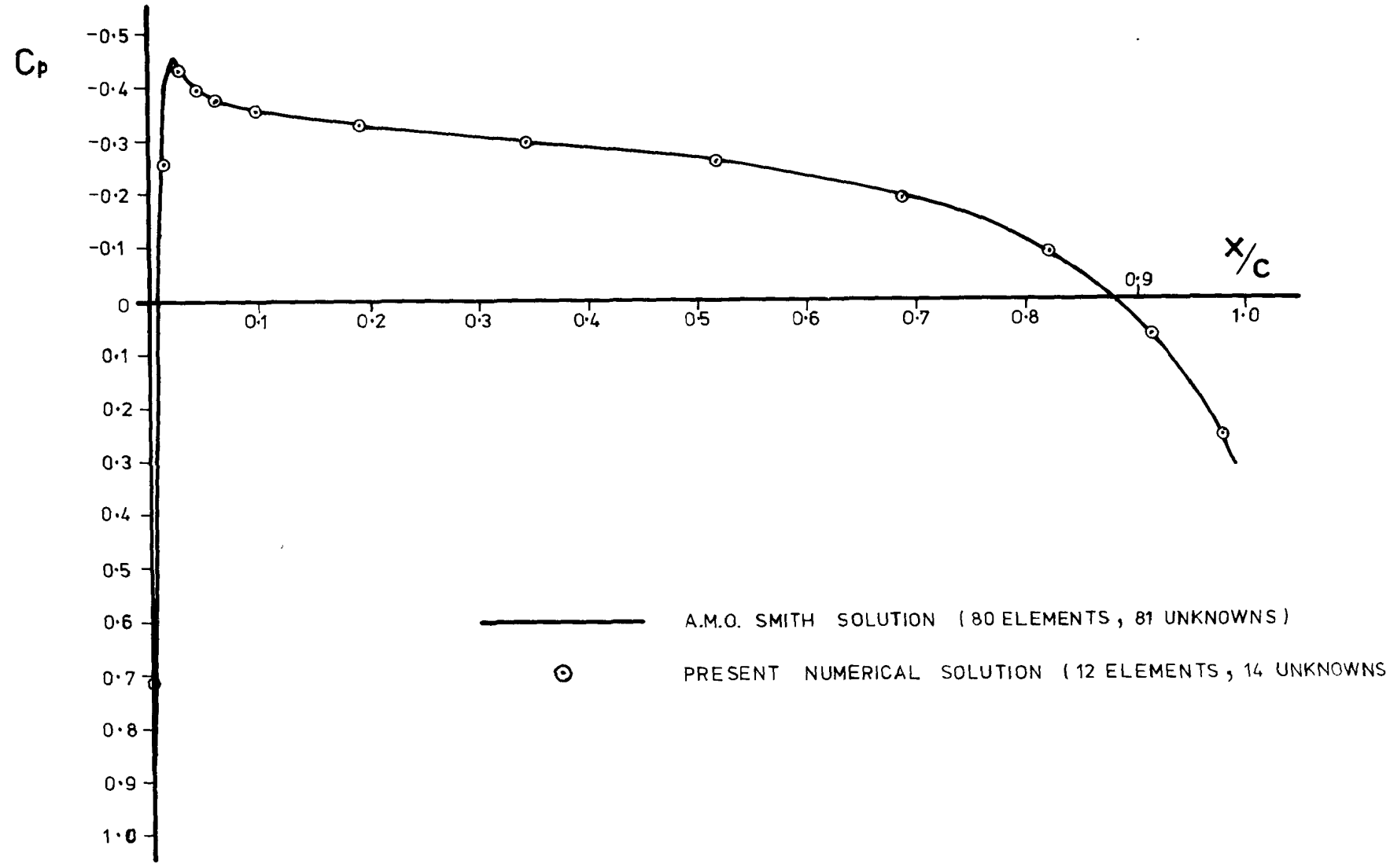

COMPARISON OF PRESENT NUMERICAL SOLUTION WITH THE A.M.O. SMITH SOLUTION

NLR AEROFOIL AT 0° INCIDENCE

Fig. 15

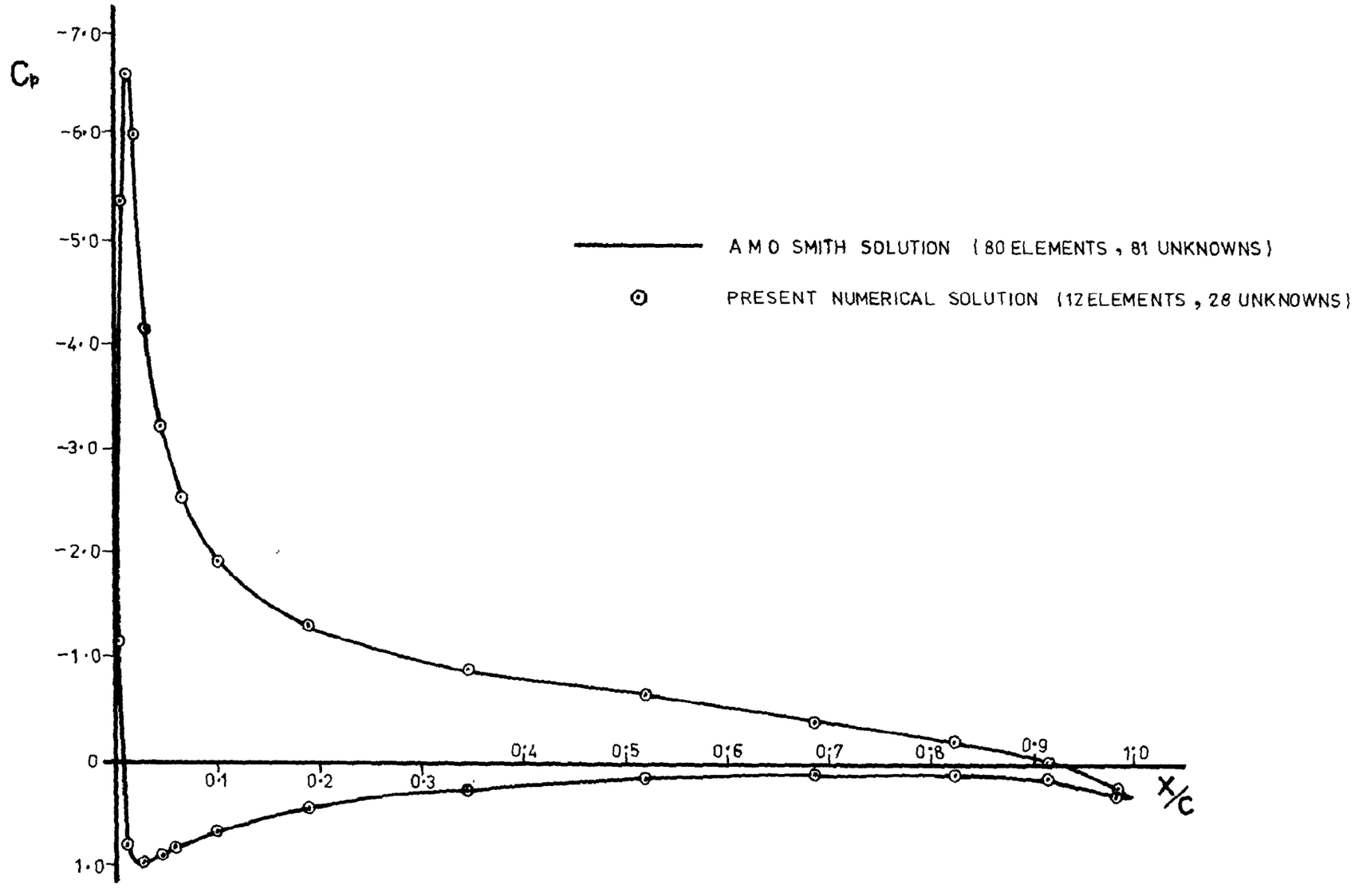

COMPARISON OF PRESENT NUMERICAL SOLUTION WITH THE A.M.O. SMITH SOLUTION
NLR AEROFOIL AT 10° INCIDENCE

Fig. 16

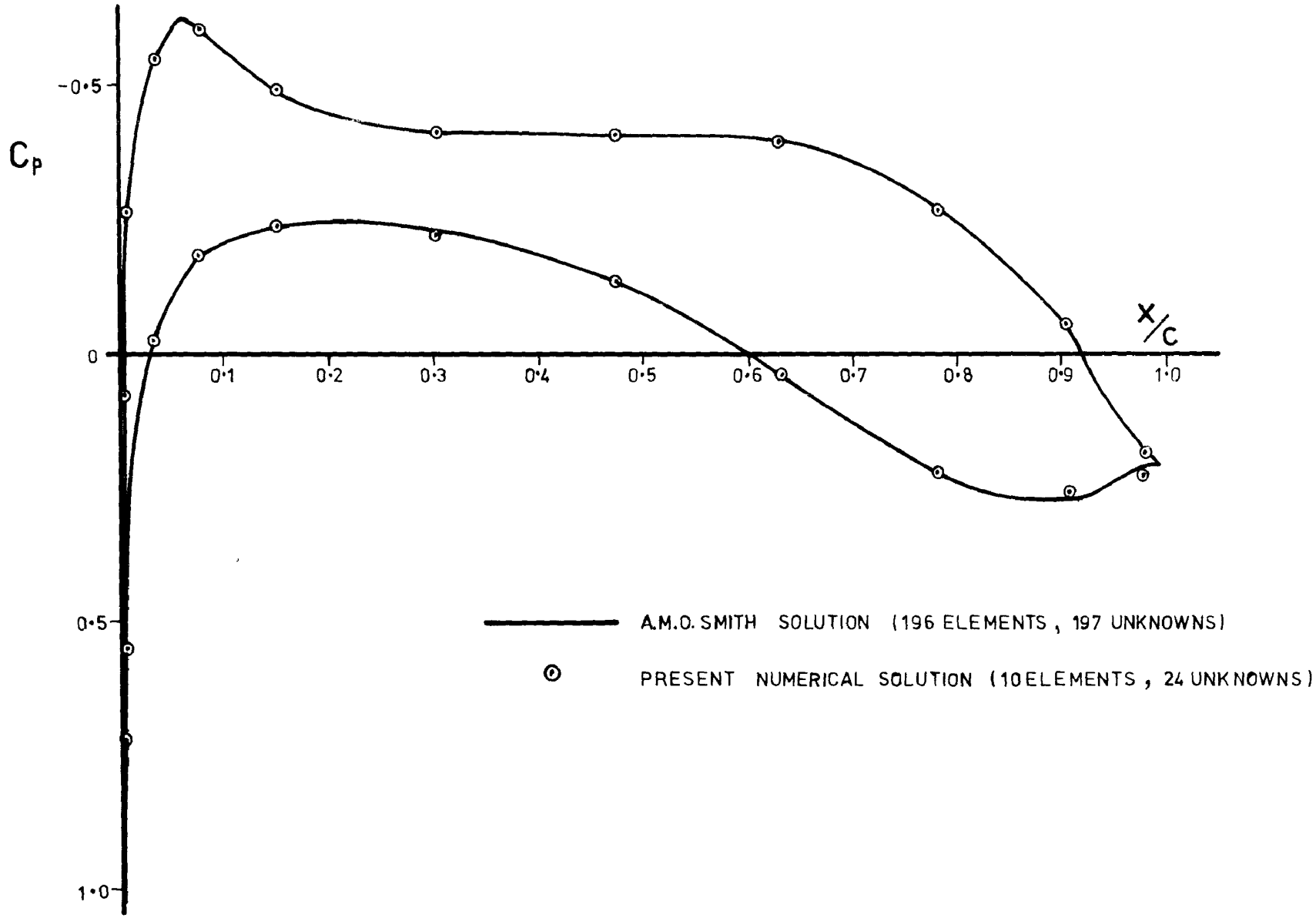

COMPARISON OF PRESENT NUMERICAL SOLUTION WITH THE A.M.O. SMITH SOLUTION GARABADIAN-KORN AEROFOIL AT 0° INCIDENCE

Fig. 17

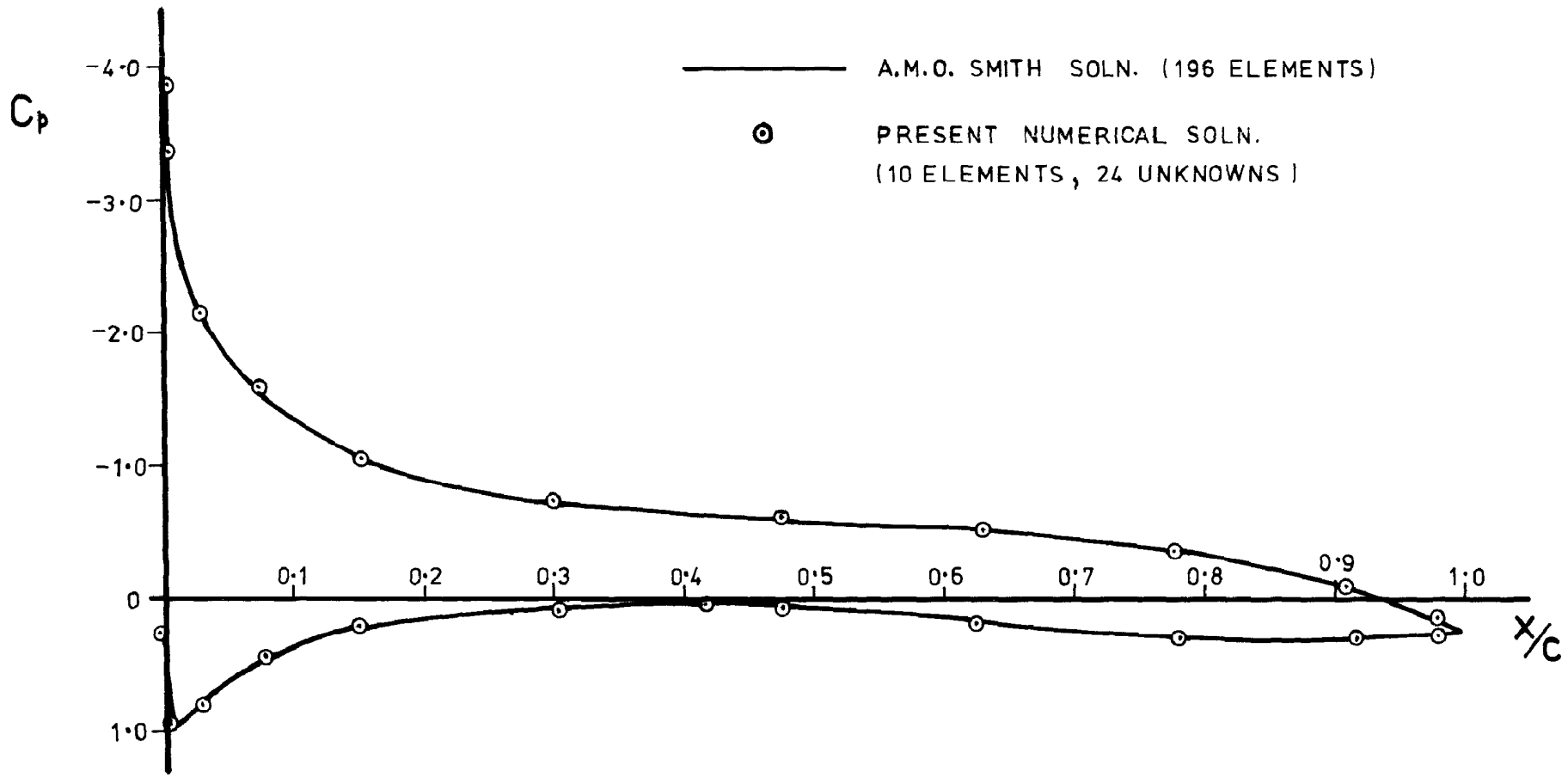

COMPARISON OF PRESENT NUMERICAL SOLUTION WITH THE A.M.O. SMITH SOLUTION

GARABADIAN-KORN AEROFOIL AT 5° INCIDENCE

Fig. 18

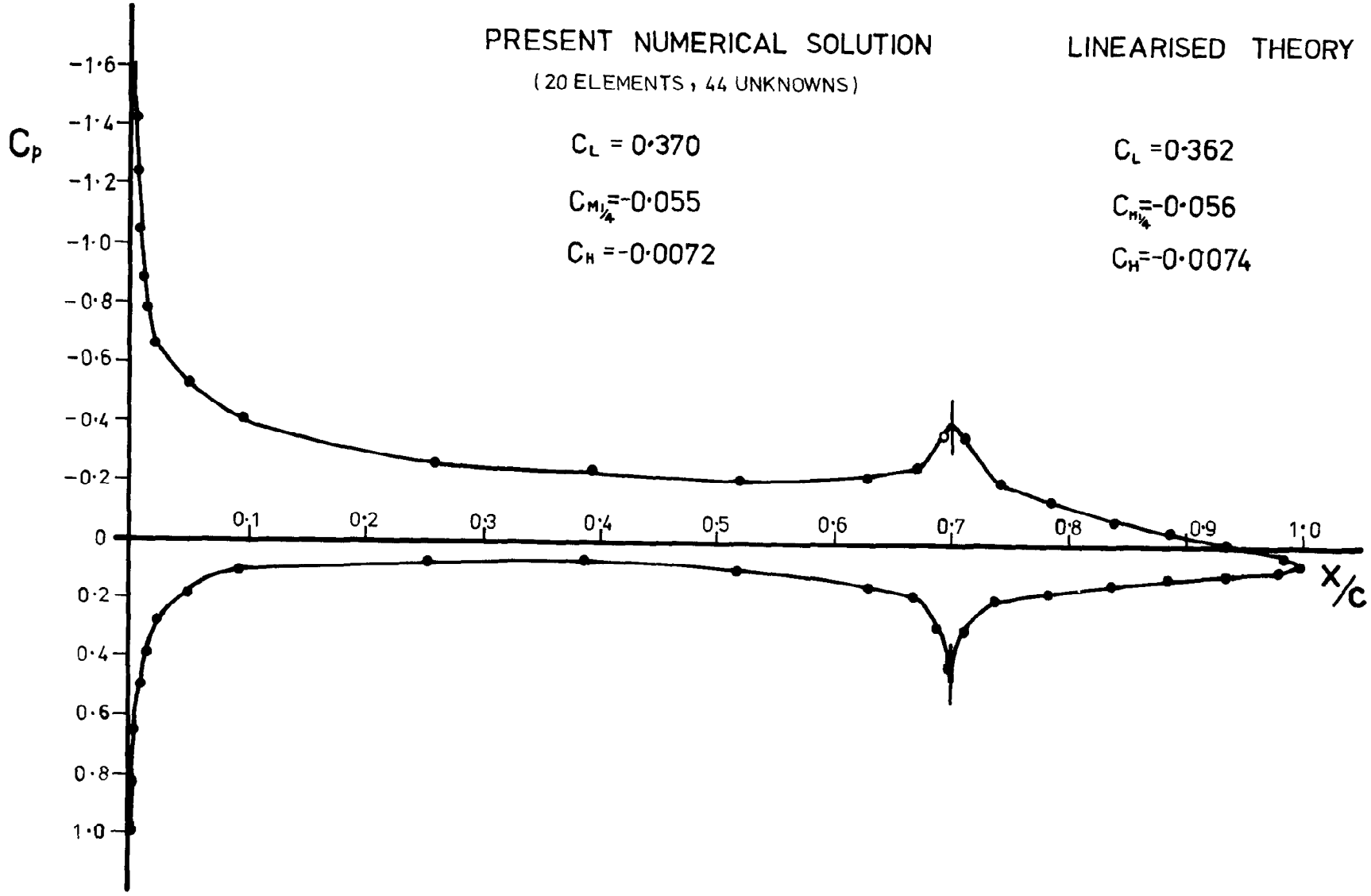

4% THICK SYMMETRICAL JOUKOWSKI AEROFOIL
30% CONTROL SURFACE CHORD $\alpha = 0$, $\delta = 5°$

Fig. 19

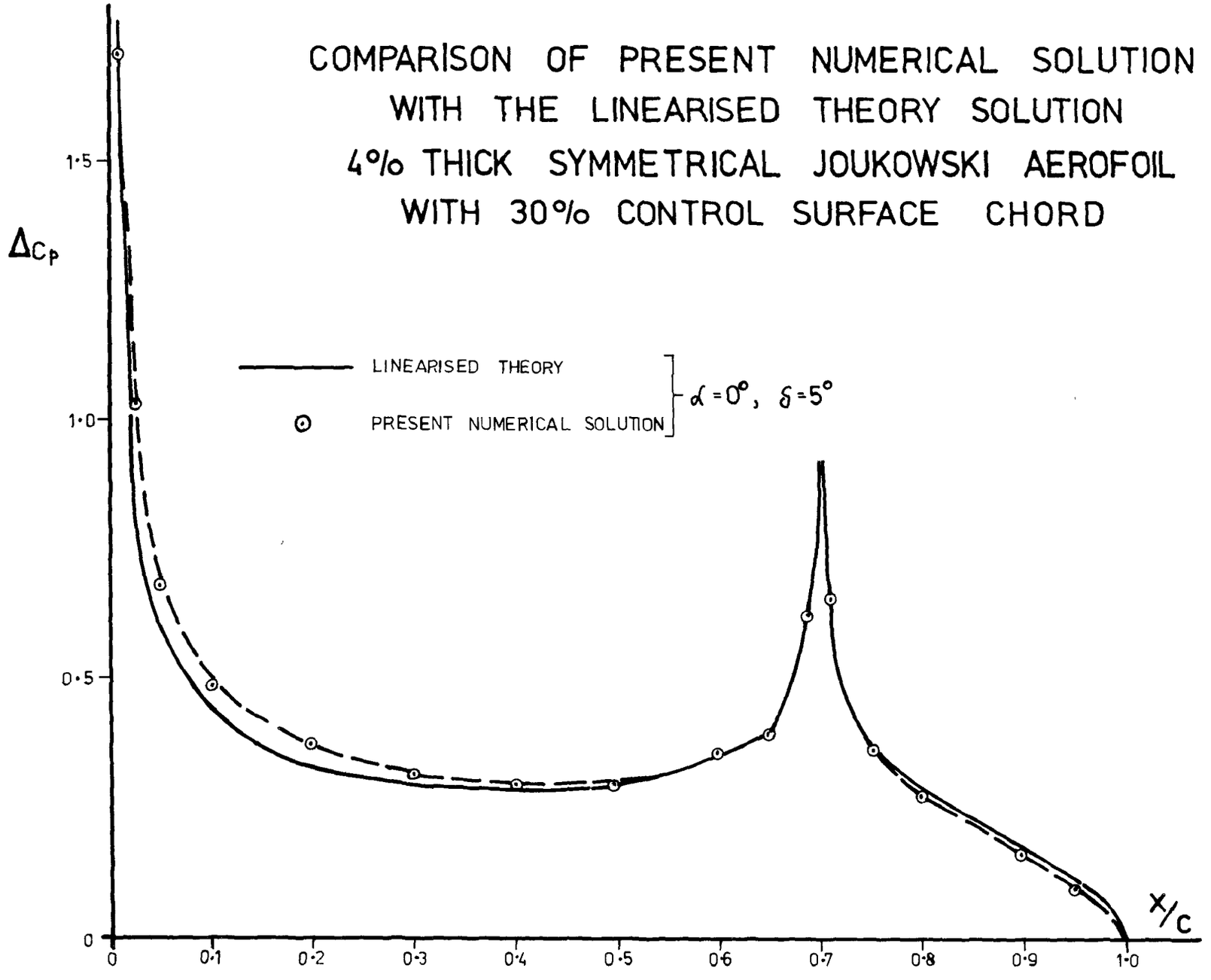
COMPARISON OF PRESENT NUMERICAL SOLUTION
WITH THE LINEARISED THEORY SOLUTION
4% THICK SYMMETRICAL JOUKOWSKI AEROFOIL
WITH 30% CONTROL SURFACE CHORD
ΔCp
1·5
1·0
0·5
0
LINEARISED THEORY
PRESENT NUMERICAL SOLUTION
α = 0°, δ = 5°
0
0·1
0·2
0·3
0·4
0·5
0·6
0·7
0·8
0·9
1·0
X/C

Fig. 20

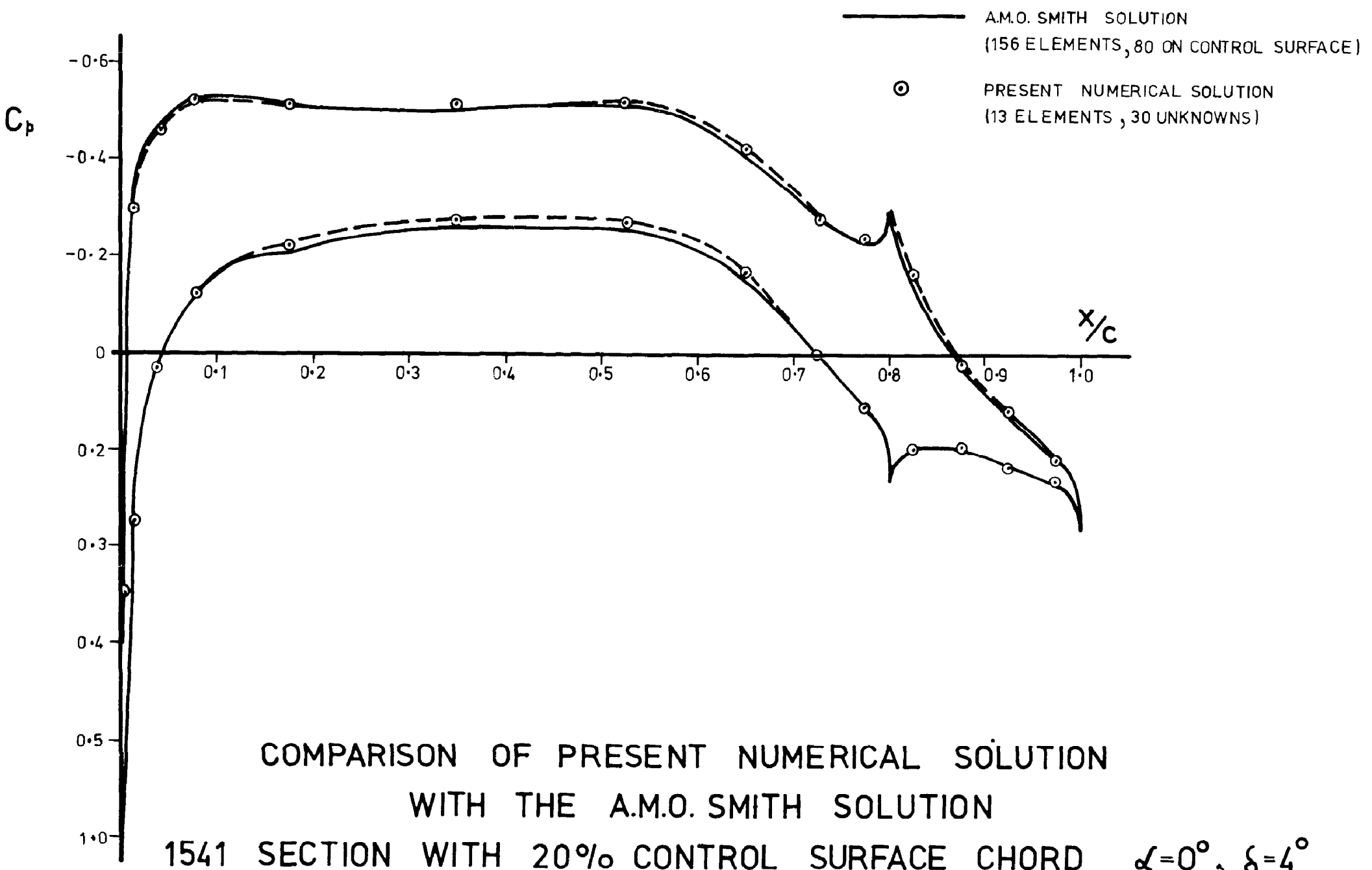

COMPARISON OF PRESENT NUMERICAL SOLUTION WITH THE A.M.O. SMITH SOLUTION

1541 SECTION WITH 20% CONTROL SURFACE CHORD $\alpha = 0°$, $\delta = 4°$

Fig. 21

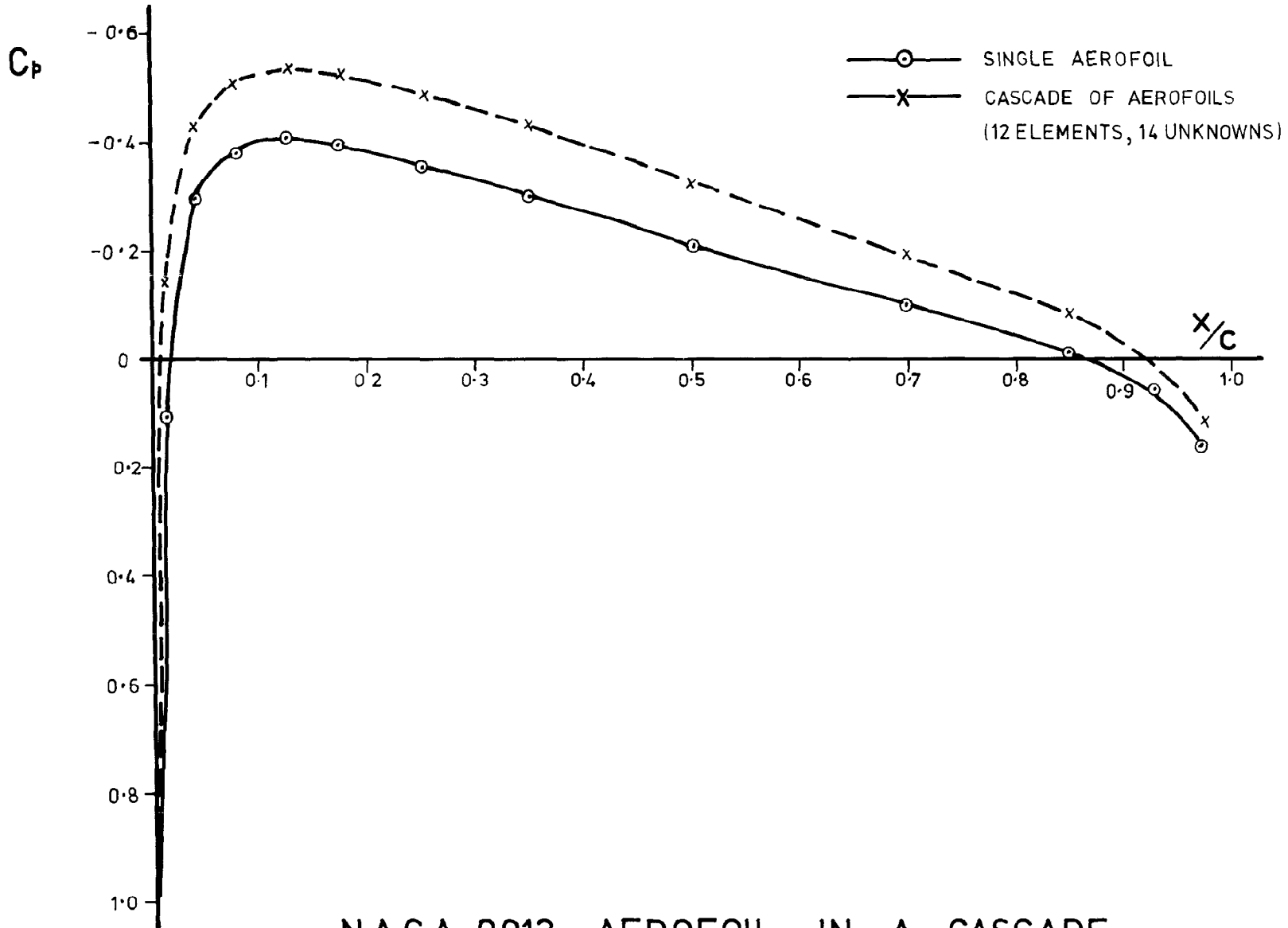

NACA 0012 AEROFOIL IN A CASCADE
0° INCIDENCE AND 0° STAGGER SPACING ONE CHORD LENGTH

Fig. 22

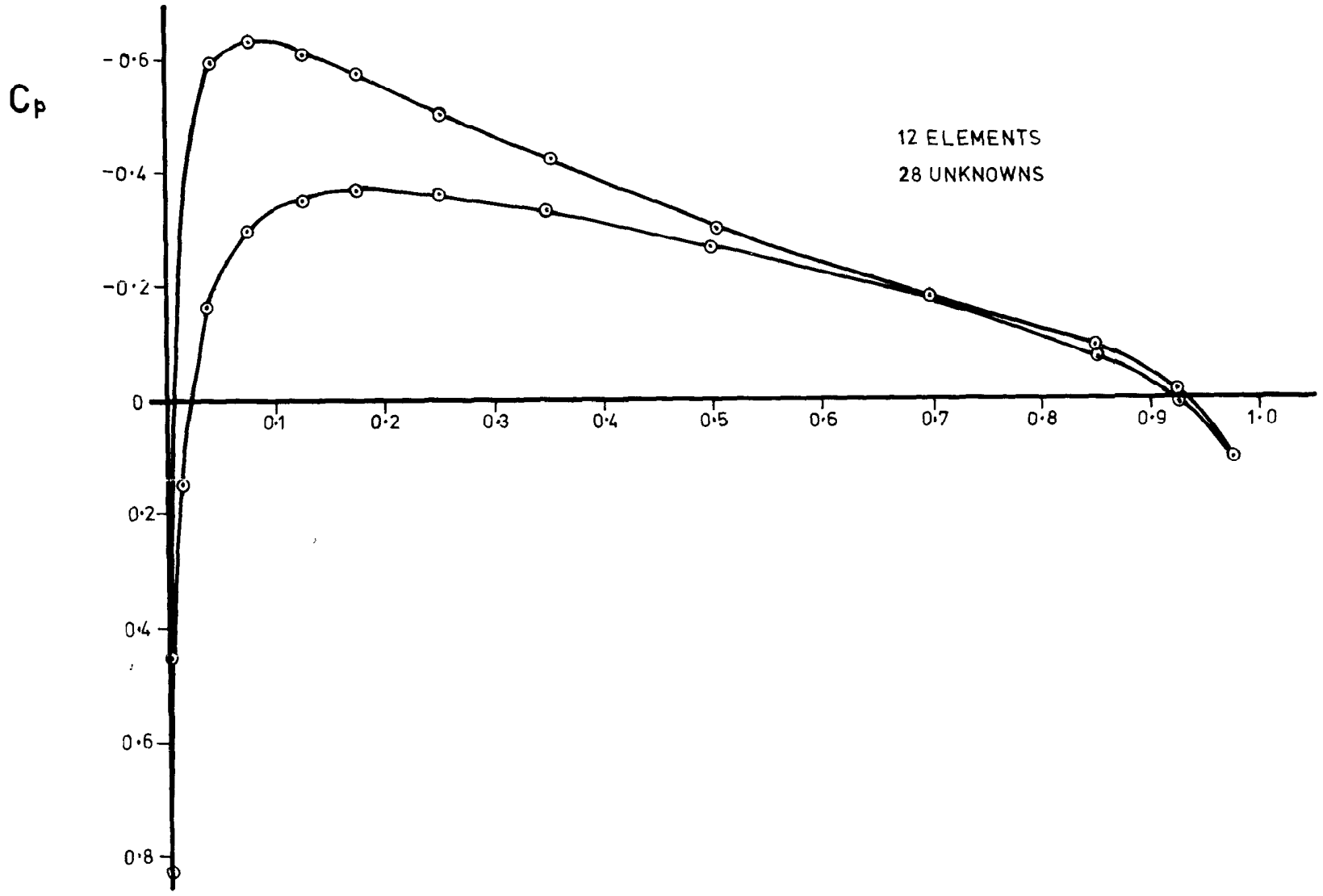

NACA 0012 AEROFOIL IN A CASCADE

0° INCIDENCE , 30° STAGGER SPACING ONE CHORD LENGTH

Fig. 23

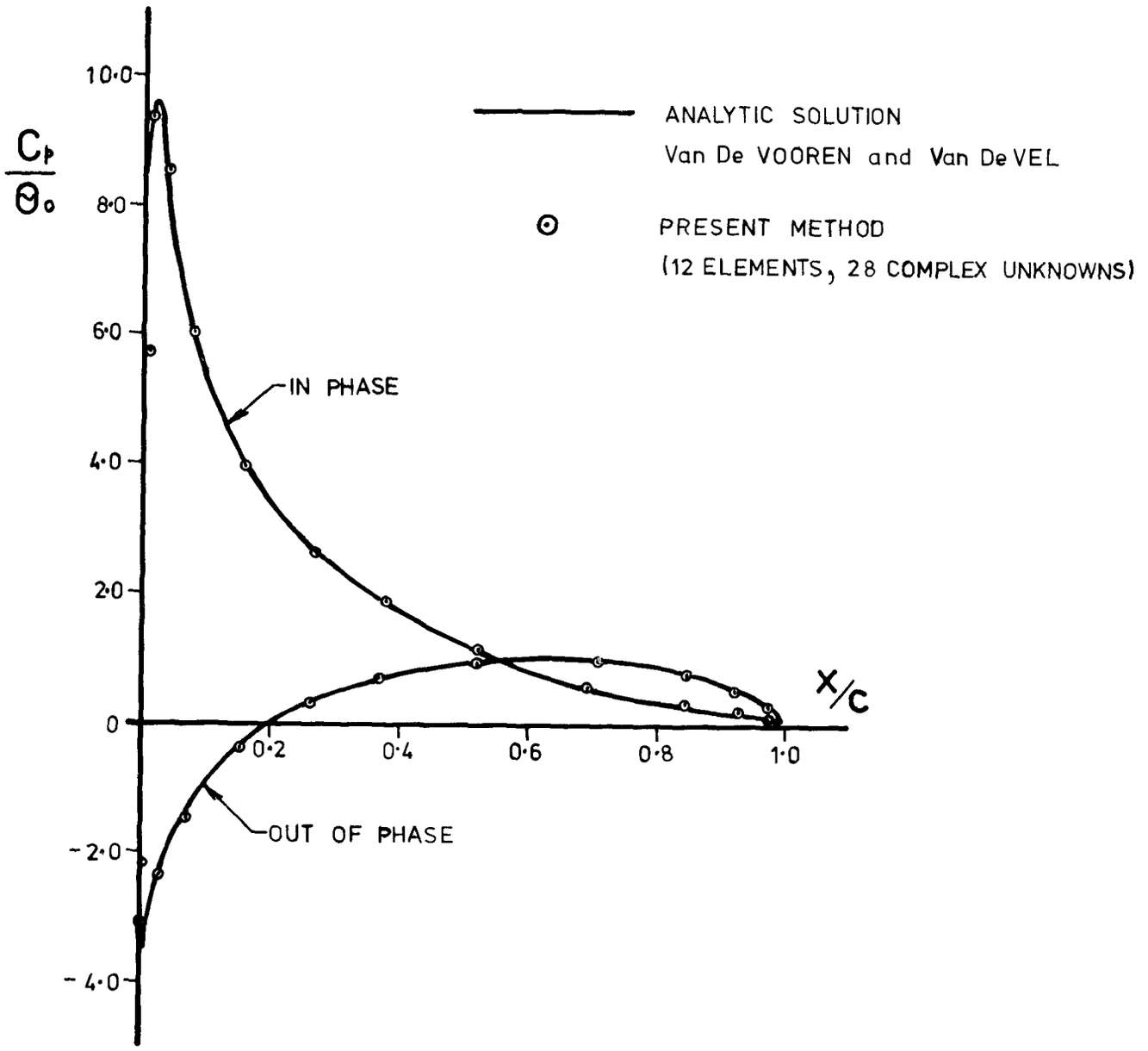

OSCILLATING AEROFOIL

$\alpha = 0°$, $\nu = 0{\cdot}8$

Fig. 24

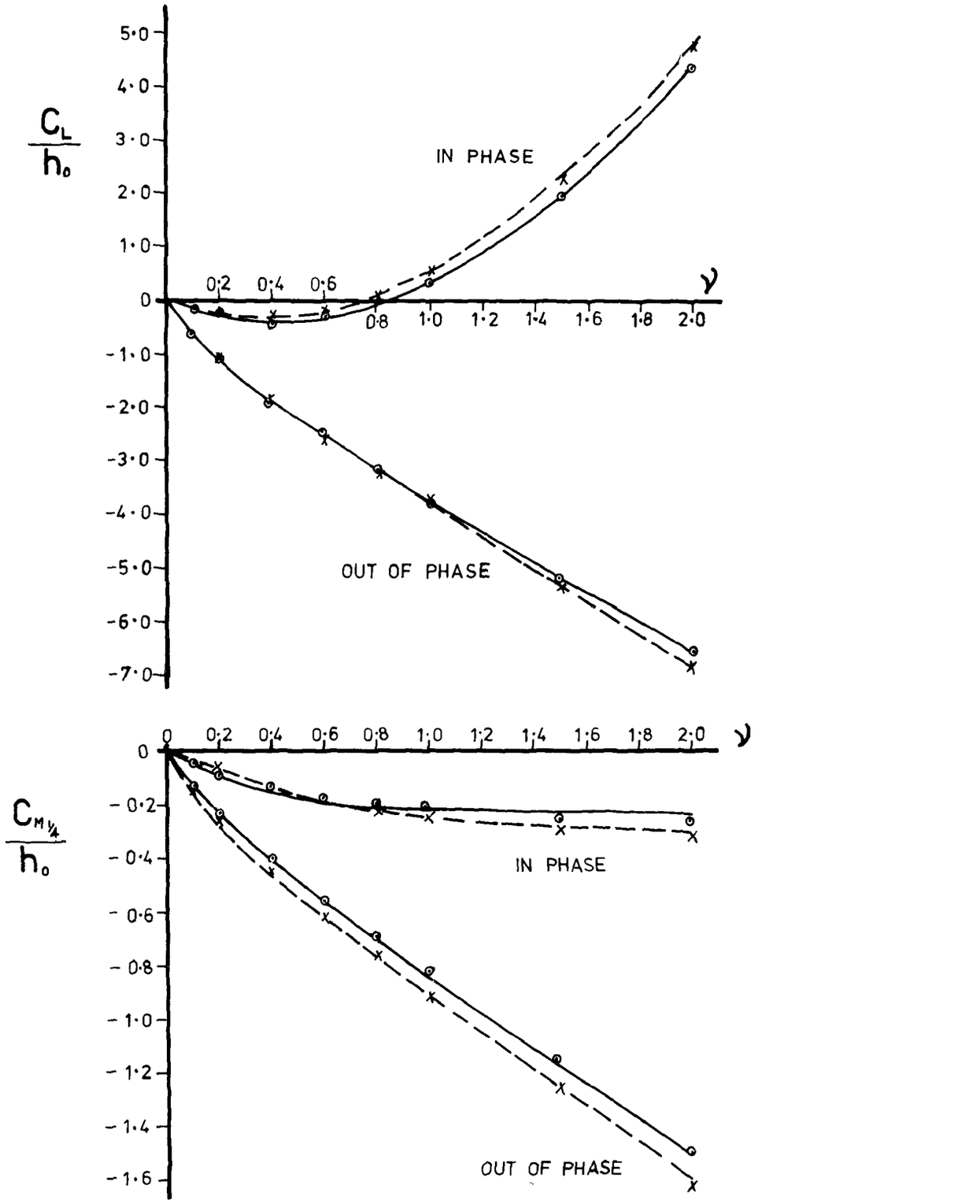

HEAVING OSCILLATION AT 0° INCIDENCE

Fig. 25

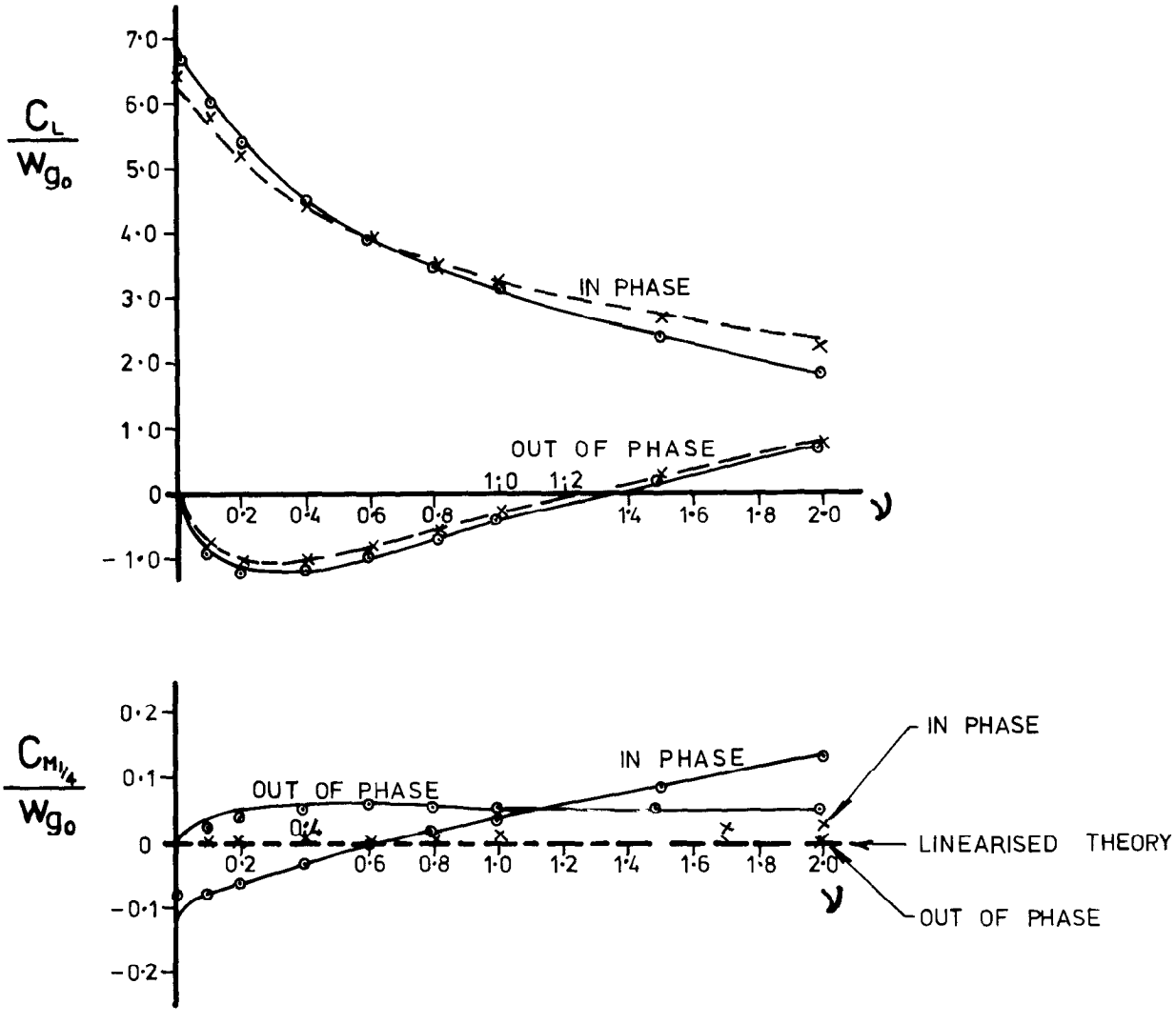

LINEARISED THEORY

X X X PRESENT METHOD, 4% JOUKOWSKI (20 ELEMENTS, 44 COMPLEX UNKNOWNS)

8·4% Von MISES
- A.M.O. SMITH (72 ELEMENTS, 73 COMPLEX UNKNOWNS)
- PRESENT METHOD (11 ELEMENTS, 26 COMPLEX UNKNOWNS)

SINUSOIDAL GUST RESPONSE

Fig. 26

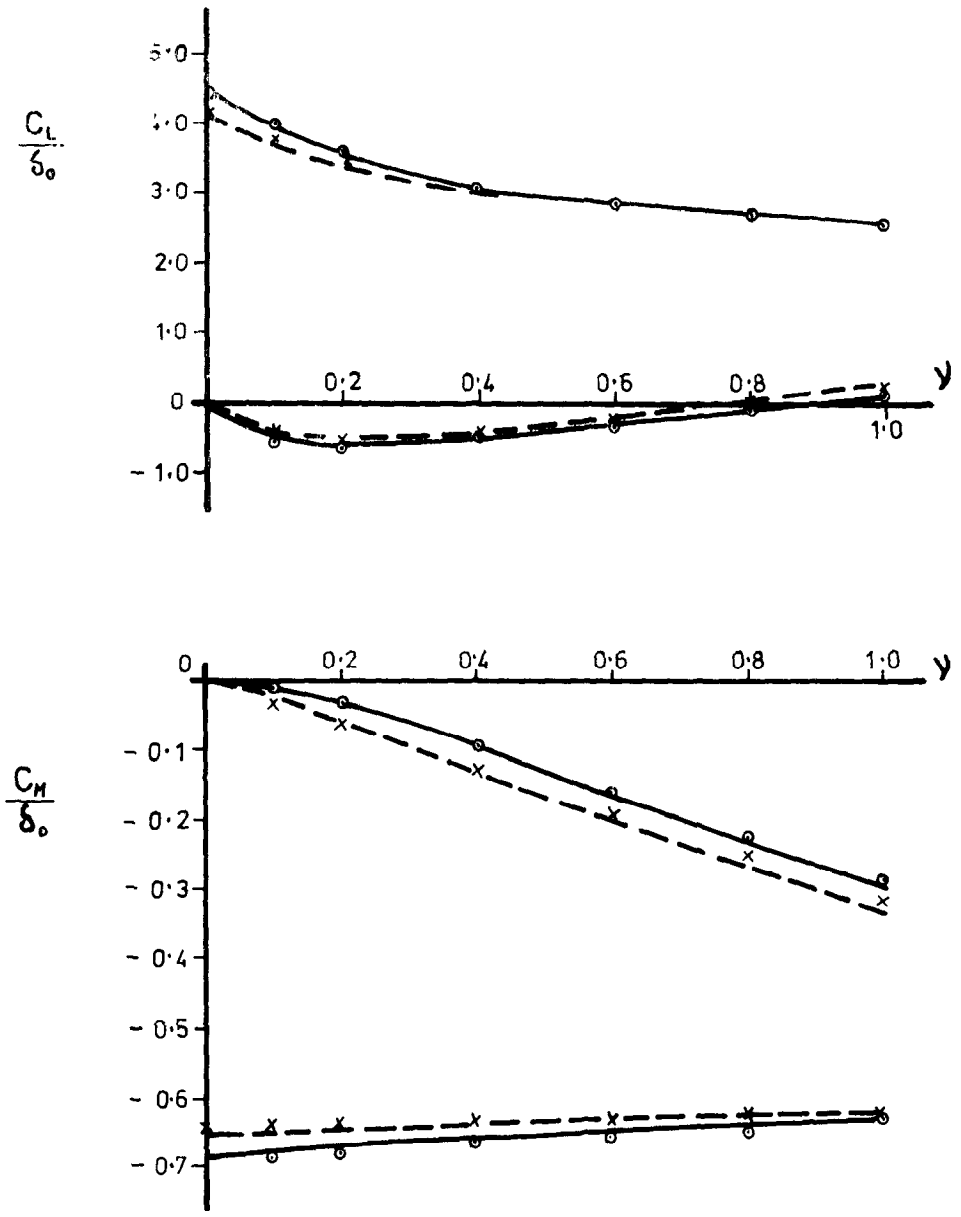

— — — — LINEARISED THEORY

× × × PRESENT METHOD 4% JOUKOWSKI (40 ELEMENTS, 84 COMPLEX UNKNOWNS)

⊙ ⊙ ⊙ KARMAN-TREFFTZ
- A.M.O. SMITH (120 ELEMENTS, 121 COMPLEX UNKNOWNS)
- PRESENT METHOD (14 ELEMENTS, 32 COMPLEX UNKNOWNS)

OSCILLATING CONTROL SURFACE

$$\left(\frac{\text{control surface chord}}{\text{aerofoil chord}} = 0{\cdot}3\right)$$

Fig. 27

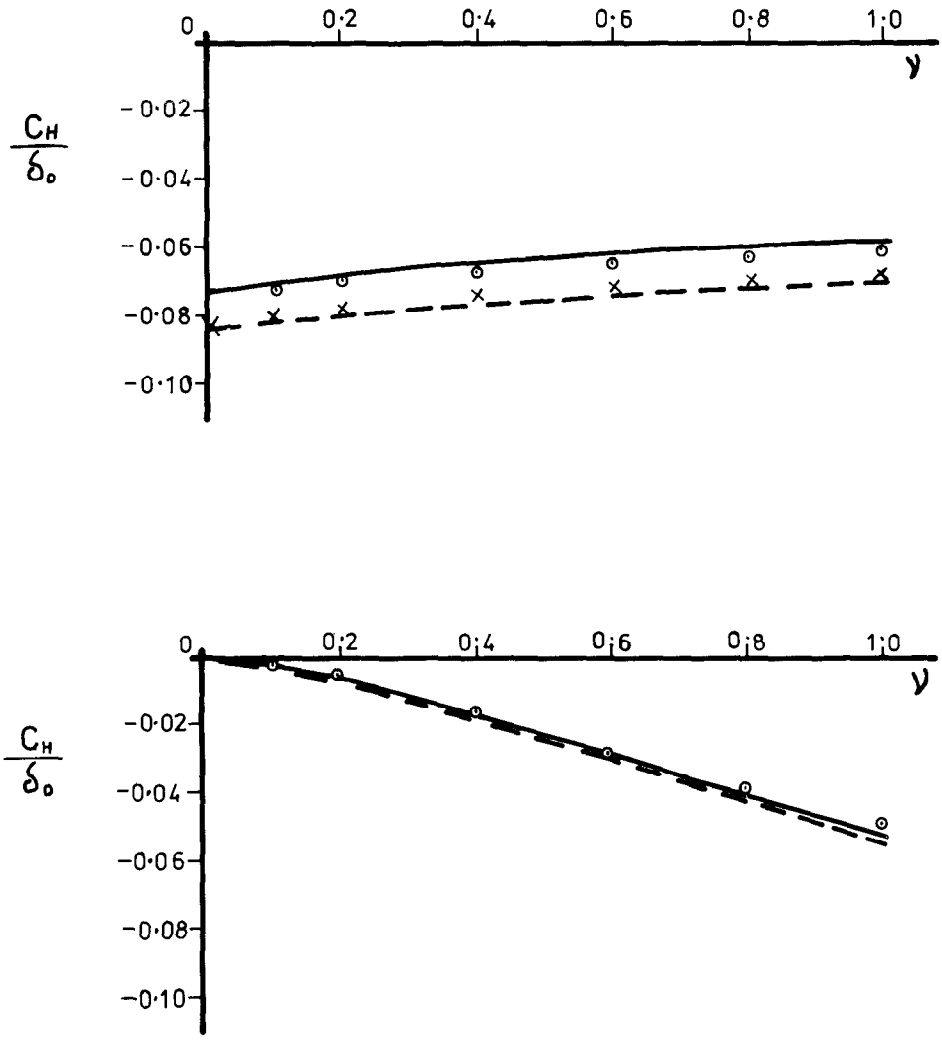

— — — — LINEARISED THEORY

× × × PRESENT METHOD 4% JOUKOWSKI (40 ELEMENTS, 84 COMPLEX UNKNOWNS)

——— KARMAN-TREFFTZ { A.M.O. SMITH (120 ELEMENTS, 121 COMPLEX UNKNOWNS)

⊙ ⊙ ⊙ { PRESENT METHOD (14 ELEMENTS, 32 COMPLEX UNKNOWNS)

OSCILLATING CONTROL SURFACE

$$\left(\frac{\text{control surface chord}}{\text{aerofoil chord}} = 0{\cdot}3\right)$$

Fig. 28

Produced in England by Her Majesty's Stationery Office, Reprographic Centre, Basildon

Bas 45228/587483 K4 2/78 P

ARC CP No. 1391
October 1976

Basu, B.C.

A MEAN CAMBERLINE SINGULARITY METHOD FOR TWO-DIMENSIONAL STEADY AND OSCILLATORY AEROFOILS AND CONTROL SURFACES IN INVISCID INCOMPRESSIBLE FLOW

A numerical method has been developed to calculate the pressure distribution on the surface of steady and oscillating aerofoils in incompressible inviscid flow. In this method singularities are placed on the mean camber line of the aerofoil and the boundary condition of/

ARC CP No. 1391
October 1976

Basu, B.C.

A MEAN CAMBERLINE SINGULARITY METHOD FOR TWO-DIMENSIONAL STEADY AND OSCILLATORY AEROFOILS AND CONTROL SURFACES IN INVISCID INCOMPRESSIBLE FLOW

A numerical method has been developed to calculate the pressure distribution on the surface of steady and oscillating aerofoils in incompressible inviscid flow. In this method singularities are placed on the mean camber line of the aerofoil and the boundary condition of/

ARC CP No. 1391
October 1976

Basu, B.C.

A MEAN CAMBERLINE SINGULARITY METHOD FOR TWO-DIMENSIONAL STEADY AND OSCILLATORY AEROFOILS AND CONTROL SURFACES IN INVISCID INCOMPRESSIBLE FLOW

A numerical method has been developed to calculate the pressure distribution on the surface of steady and oscillating aerofoils in incompressible inviscid flow. In this method singularities are placed on the mean camber line of the aerofoil and the boundary condition of/

ARC CP No. 1391
October 1976

Basu, B.C.

A MEAN CAMBERLINE SINGULARITY METHOD FOR TWO-DIMENSIONAL STEADY AND OSCILLATORY AEROFOILS AND CONTROL SURFACES IN INVISCID INCOMPRESSIBLE FLOW

A numerical method has been developed to calculate the pressure distribution on the surface of steady and oscillating aerofoils in incompressible inviscid flow. In this method singularities are placed on the mean camber line of the aerofoil and the boundary condition of/

of tangency of flow is satisfied on the surface of the aerofoil. Problems considered include steady single aerofoils with and without control surfaces, a cascade of aerofoils, aerofoils oscillating in pitch, aerofoils oscillating in heave, aerofoils in harmonic travelling gusts and control surface oscillations. Comparison with analytic solutions, and other numerical methods, where available, are good. The main advantages of this method are the relatively fast computing times and the fact that the method converges satisfactorily in the limit of zero aerofoil thickness.	of tangency of flow is satisfied on the surface of the aerofoil. Problems considered include steady single aerofoils with and without control surfaces, a cascade of aerofoils, aerofoils oscillating in pitch, aerofoils oscillating in heave, aerofoils in harmonic travelling gusts and control surface oscillations. Comparison with analytic solutions, and other numerical methods, where available, are good. The main advantages of this method are the relatively fast computing times and the fact that the method converges satisfactorily in the limit of zero aerofoil thickness.
of tangency of flow is satisfied on the surface of the aerofoil. Problems considered include steady single aerofoils with and without control surfaces, a cascade of aerofoils, aerofoils oscillating in pitch, aerofoils oscillating in heave, aerofoils in harmonic travelling gusts and control surface oscillations. Comparison with analytic solutions, and other numerical methods, where available, are good. The main advantages of this method are the relatively fast computing times and the fact that the method converges satisfactorily in the limit of zero aerofoil thickness.	of tangency of flow is satisfied on the surface of the aerofoil. Problems considered include steady single aerofoils with and without control surfaces, a cascade of aerofoils, aerofoils oscillating in pitch, aerofoils oscillating in heave, aerofoils in harmonic travelling gusts and control surface oscillations. Comparison with analytic solutions, and other numerical methods, where available, are good. The main advantages of this method are the relatively fast computing times and the fact that the method converges satisfactorily in the limit of zero aerofoil thickness.

HER MAJESTY'S STATIONERY OFFICE

Government Bookshops

49 High Holborn, London WC1V 6HB
13a Castle Street, Edinburgh EH2 3AR
41 The Hayes, Cardiff CF1 1JW
Brazennose Street, Manchester M60 8AS
Southey House, Wine Street, Bristol BS1 2BQ
258 Broad Street, Birmingham B1 2HE
80 Chichester Street, Belfast BT1 4JY

Government publications are also available through booksellers

C.P. No. 1391

ISBN 0 11 471137 2